Photoluminescence Studies of Synthesized Condensed Thiophene Analogue of Angelicin, Stilbene and Dibenz[c,h]acridine Derivatives to Explore Their Applicability: Effect of Heteroarene Substituents

Summary of Work (5000 words)

For the Award of Ph.D. (Sc.) Degree in Chemistry

Submitted to

Department of Chemistry, Presidency University,

86/1 College Street, Kolkata-700073

By

TUYAN BISWAS

Registration No: R-18RS205270166 dated 28th November 2019

Under the Joint Supervision of

Dr. Arnab Halder

Professor of Chemistry,
Department of Chemistry,

Presidency University,
86/1 College Street,
Kolkata-700073

Dr. Gandhi Kumar Kar

Professor (Rtd.) of Chemistry,
Department of Chemistry,

Presidency University,
86/1 College Street,
Kolkata-700073

Acknowledgement

I extend my deepest gratitude to my supervisor and mentor, **Professor Arnab Halder**, whose inspiring and patient guidance has been a beacon throughout this challenging journey. His profound knowledge, invaluable suggestions, and warm encouragement have illuminated my path as I pursued the truth.

Heartfelt thanks go to my co-supervisor, **Professor (now Retired) Gandhi Kumar Kar**, for his indispensable advice, patient guidance, and unwavering support. His profound knowledge in chemical synthesis has greatly enriched my understanding.

I express sincere appreciation to **Dr. Debrani Mitra**, Assistant Professor in the Department of Life Science, Presidency University, Kolkata, for her constant support.

I extend my thanks to my seniors and all colleagues in our group for their encouragement and assistance. Special appreciation goes to the non-teaching staffs of the Department of Chemistry, PU for their technical supports.

I reserve my gratitude for my parents, my sister Tiyan, and my husband, for their love, understanding, encouragement, and unwavering supports.

Finally, I would like to acknowledge all those who contributed to my journey during the period of my studies on this research work. Your collective support has been instrumental in my success.

Contents

The thesis, titled **"Photoluminescence Studies of Synthesized Condensed Thiophene Analogue of Angelicin, Stilbene and Dibenz[c, h]acridine Derivatives to Explore Their Applicability: Effect of Heteroarene Substituents"** provides a comprehensive overview of the varied synthetic strategies employed for the methyl derivatives of thieno-angelicin, thieno-stilbene, and thieno-acridine. These derivatives are synthesized from a common starting material, α-β unsaturated chloraldehyde, and the thesis focuses on conducting fluorescence studies to investigate their interactions, primarily with various solvents to check their applicability.

The thesis is organized into three chapters, each with detailed subdivisions. **Chapter I** is further divided into five subsections: **IA**, **IB**, **IC**, **ID**, and **IE**. **Chapter II** is segmented into **IIA** and **IIB**, while **Chapter III** encompasses **IIIA**, **IIIB**, and **IIIC**. Through these chapters and subsections, the thesis delves into the synthesis processes, and the photoluminescent behavior of the synthesized compounds.

Chapter I: Thiophene analogue of angelicin derivative: ethyl 8-methyl-2-oxo-2H-thieno[2,3-h]chromene-3-carboxylate (MTCE)

IA. Synthesis of MTCE

IB. Fluorescence studies on the interaction of MTCE with solvents

IC. Fluorescence studies on the interaction of MTCE with BSA protein

ID. Fluorescence studies on the interaction of MTCE with metal ions

IE. Fluorescence studies on the interaction of MTCE with β-Cyclodextrin

Chapter II: Thiophene analogue of stilbene derivative: (*E*)-1,2-bis(2-methylbenzo[1,2-b:3,4-b']dithiophen-7-yl)ethene (MTS)

IIA. Synthesis of MTS

IIB. Fluorescence studies on the interaction of MTS with solvents

Chapter III: Thiophene analogue of acridine derivative: 2-methylbenzo[c]thieno[3,2-h]acridine (MTA)

IIIA. Synthesis of MTA

IIIB. Fluorescence studies of MTA in pure and binary solvents

IIIC. Fluorescence studies of acido-chromic behaviour of MTA

Chapter I: Thiophene analogue of angelicin derivative: ethyl 8-methyl-2-oxo-2H-thieno[2,3-h]chromene-3-carboxylate (MTCE)

Introduction

Angelicin, an angularly fused parent furanocoumarin, has been employed since ancient times and is naturally present in plants like Apiaceae and Fabaceae.[1] Angelicin, exhibiting photosensitivity, exclusively forms monoadducts with DNA upon exposure to UV radiation. This unique property has positioned it as a compelling candidate in phototherapy, owing to its capacity to create easily repairable monoadduct with DNA.[2-4] Furthermore, angelicin has demonstrated versatile therapeutic properties, including anti-cancer, anti-viral, anti-inflammatory, anti-microbial effects, as well as the promotion of pro-osteogenic and chondrogenic differentiation, along with erythroid differentiating properties.[5-9] Angelicin and its derivatives have appeared as promising compounds for many research groups due to their therapeutic properties. However, there are few reports on the chemical synthesis of thiophene analogues of angelicin and its derivatives.[1] Bordin *et al.* have elucidated the synthesis of angelicin using benzofuran synthons, exemplified by the karanjol derivative.[10] The synthesis of Angelicin, as presented by Aneja *et al.* commences with Umbelliferone (the BC ring precursor).[11] In 1998, Louisa Mosti *et al.* reported a four-step synthesis of thia-angelicin from a bicyclic enaminoketone.[12] Ana P. Esteves *et al.* reported the synthesis of benzopsoralen and benzoangelicin derivatives, along with their thiophene and pyrrole analogues.[13] The inhibitory effects on the growth of tumor cell lines (MDA, MB231 and TCC-SUP) were assessed. Although the compounds exhibited anti-proliferative activity, the highest efficacy was observed in the benzopsoralen derivative. Prompted by the imperative need to attempt the synthesis of a thiophene analogue of Angelicin and investigate its biological activity, we initiated the present study focused on synthesizing 8-methyl-2H-thieno[2,3-h]chromen-2-one as a derivative resembling Angelicin with a thiophene moiety. We introduce an efficient and high-yielding total synthesis strategy for a novel thieno-angelicin derivative (MTCE), achieved in four steps starting from β-chloro-α,β-unsaturated aldehyde.

Many coumarin derivatives display significant Stokes shifts, attributed to the substantial disparity between their ground and excited state dipole moments. These shifts exhibit high sensitivity to solvent polarity and environmental conditions.[14-17] Our synthesized thiophene-fused coumarin derivative, MTCE, demonstrates solvatochromism in variously polar solvents. With an escalation in solvent polarity, the emission corresponding to the $\pi^* \rightarrow \pi$ transition

experiences an almost 60 nm redshift. This phenomenon is attributed to the formation of a more polar excited state, leading to the redistribution of π electrons between the thiophene and coumarin nucleus. The ground and excited state dipole moments were determined experimentally using the solvatochromic shift method with the help of three independent equations proposed by Lippert,[18] Bakshiev,[19] and Bilot–Kawski.[20-21] This study establishes a foundation for future inquiries into thienoangelicin derivatives as solvatochromic probes, offering insights into the dynamics of biological organelles, facilitating the study of disease models, and inspiring the design of nonlinear optoelectronic materials.

The interaction between drugs and proteins is extensively explored using serum albumin, a major soluble constituent in the circulatory system.[22-23] Bovine Serum Albumin (BSA) is particularly valuable for investigating drug-protein interactions due to its structural homology with Human Serum Albumin (HSA) and its high conformational adaptivity.[24] Among its 582 amino acids, BSA features only two tryptophan regions: Trp-134 in the eighth helix in domain I (subdomain IA) and Trp-213 in the second helix in domain II (subdomain IIA).[25-26] Alterations in the intrinsic tryptophan fluorescence in the presence of an exogenous substance provide valuable insights into the binding nature of the ligand-protein system. A well-established methodology has been employed to elucidate the interactions in the ligand-protein system.[14, 27-28] Our recently synthesized MTCE was employed to investigate its interaction with Bovine Serum Albumin (BSA) by monitoring tryptophan emission, providing additional insights into the binding mechanism and thermodynamic parameters. The study encompassed a comprehensive approach, including UV-vis spectra analysis, synchronous fluorescence, circular dichroism spectra, molecular docking, and site-marker competitive experiments, all contributing to the validation of our findings.

The utilization of fluorescence probes for metal ion detection in biosystems and the environment has garnered substantial attention, owing to their rapid and selective sensing capabilities with simple instrumentation.[29-30] In recent years, various coumarin derivatives have been explored for detecting different metal ions.[31-32] Our newly synthesized thienoangelicin derivatives demonstrate noteworthy 'off-sensing' fluorescence selectivity specifically toward Fe^{3+} ions, achieving a remarkable detection limit as low as 0.35 μM. Given the pivotal role of iron in biosystems, the selective sensing of this metal holds significant implications in diverse applications within biomedicine and environmental contexts.[33-34] Therefore, our findings suggest a promising application for thienoangelicin derivatives in optical sensing. The significance of this research stems from its innovative approach to

synthesizing MTCE in a highly efficient manner, opening up a range of potential applications across various fields such as therapy, optical sensing, and probing.

Chapter IA: Synthesis of MTCE

For an extended duration, Kar *et. al*. have been engaged in the synthesis of polycyclic thiophene derivatives, employing β-halo-α,β-unsaturated aldehydes as fundamental building blocks.[35] The retrosynthesis of the target molecule is depicted in **Figure 1**, revealing the successful synthesis originating from 4-chloro-2-methyl-6,7-dihydrobenzo[b]thiophene-5-carbaldehyde (**1)** a compound previously synthesized in our laboratory by following the literature procedure.[36-37]

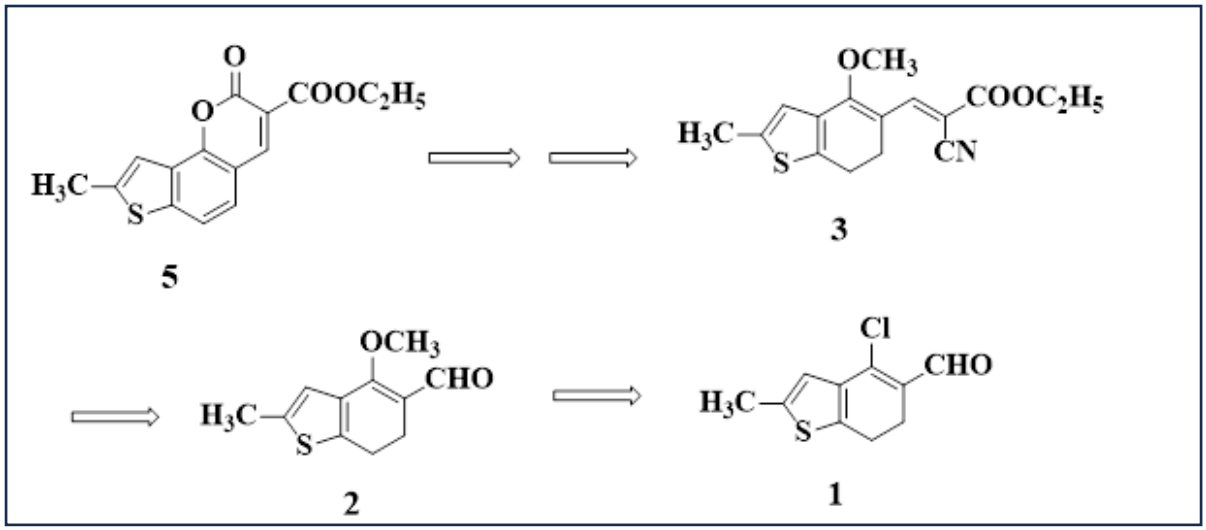

Figure 1. Retrosynthesis scheme of the thieno-angelicin derivative (MTCE).

Figure 2 illustrates the synthesis of the title compound in four steps, starting from chloraldehyde (**1**). 4-methoxy-2-methyl-6,7-dihydrobenzo[b]thiophene-5-carbaldehyde (**2**) was synthesized in 85% yield as a viscus faint orange liquid by treatment of chloraldehyde (**1**) with NaOMe/MeOH under reflux. Next, the methoxyaldehyde (**2**) was condensed with ethyl cyanoacetate in ethanol under reflux in presence of catalytic aq. KOH to yield the nitrile derivative (**3**) as a yellow solid in 82% yield. Compound (**3**) was then refluxed with pyridinium hydrochloride in quinoline for 45 minutes, resulting in cyclization to ethyl 8-methyl-2-oxo-5,6-dihydro-2H-thieno[2,3-h] chromene-3-carboxylate (**4**), which was obtained as a yellow solid in good yield. The dihydro-thienoangelicin derivative (**4**) was then aromatized (DDQ, dry

benzene, reflux, 2 hr) to produce the target compound, ethyl 8-methyl-2-oxo-2H-thieno[2,3-h]chromene-3-carboxylate (**5**), as a needle-like, faint yellow solid in 90% yield. The compounds were characterized by usual spectroscopic analysis (^{1}H-NMR, ^{13}C-NMR and HRMS). Tentative assignments of ^{1}H-NMR chemical shift (δ, ppm) and the splitting pattern of compound 2-5 have described in **Figure 3**

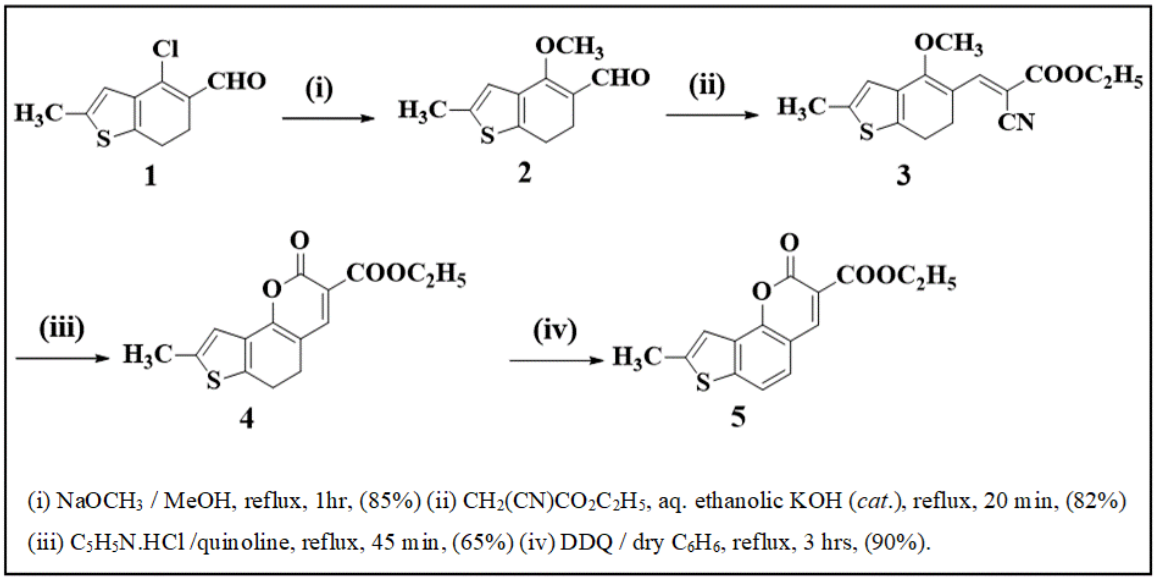

Figure 2. Synthesis of the thienoangelicin derivative, ethyl 8-methyl-2-oxo-2H-thieno[2,3-h]chromene-3-carboxylate (MTCE).

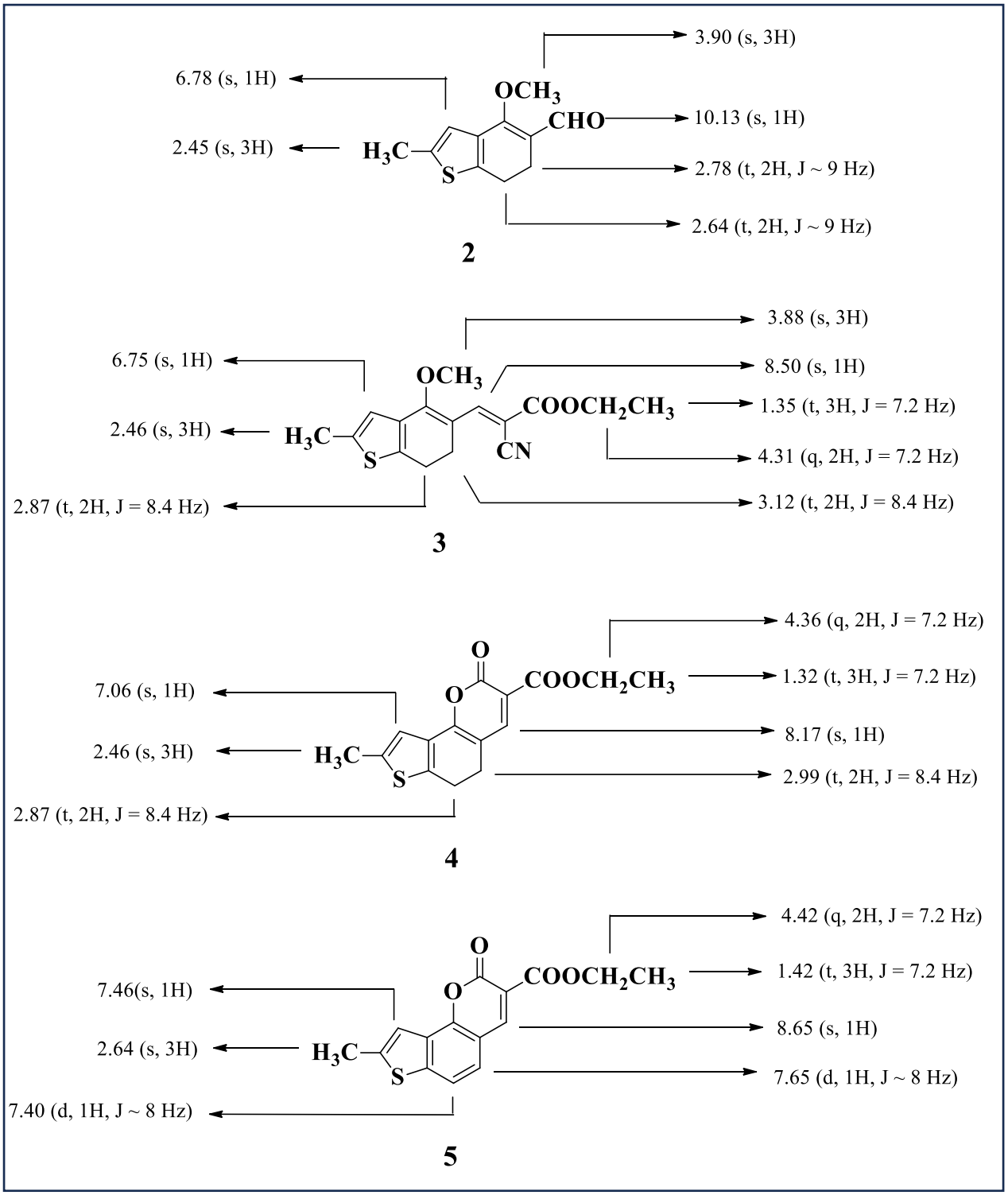

Figure 3. Tentative assignments of ^{1}H-NMR chemical shift (δ, ppm) and the splitting pattern of compound **2-5.**

Chapter IB: Fluorescence studies on the interaction of MTCE with solvents

The UV-Vis spectra of the synthesized MTCE were systematically recorded in solutions comprising ten solvents with varying dielectric constants (ε). The spectral data for MTCE are summarized in **Table 1**, while the representative UV-Vis absorption spectra in n-hexane, benzene, acetonitrile, methanol, and 1,2-dichloromethane have been illustrated in **Figure 4a**. These spectra reveal two primary absorption bands, centered around 327 nm and 365 nm, attributed to the $\pi \rightarrow \pi^*$ transition. The concentration of the MTCE (2 μM) was sufficiently diluted (OD < 0.1) to rule out solute-solute interaction in that range. The red shift in the absorption band may be due to the formation of intermolecular H-bonds between the H-bond donor solvent and MTCE, stabilizing the ground state. However, the ground state energy distribution is not affected to a greater extent due to the less polar nature of MTCE in the ground state.

Table 1. Quantum yield, solvent parameter and spectral data of MTCE in different solvents

Solvents	ε	n	λ_{abs} **(nm)**	λ_{fl} **(nm)**	$\overline{\nu_a} - \overline{\nu_f}$ **(cm^{-1})**	$\frac{\overline{\nu_a} + \overline{\nu_f}}{2}$ **(cm^{-1})**	$F(\varepsilon, n)$	$F_1(\varepsilon, n)$	$F_2(\varepsilon, n)$	φ
DMSO	46.7	1.479	331	490	9803	25309.82	0.263	0.528	0.588	0.044
CH_3CN	37.5	1.344	327	484	9920	25621.10	0.305	0.489	0.479	0.041
DMF	36.7	1.430	329	486	9819	25485.63	0.274	0.507	0.546	0.042
MeOH	32.7	1.328	330	480	9470	25568.18	0.309	0.477	0.462	0.043
EtOH	24.5	1.361	331	474	9114	25654.26	0.289	0.467	0.480	0.039
DCM	8.93	1.424	331	460	8472	25975.31	0.217	0.357	0.466	0.038
EtOAc	6.02	1.372	325	458	8935	26301.65	0.200	0.284	0.395	0.038
$CHCl_3$	4.81	1.446	333	455	8052	26004.03	0.148	0.228	0.416	0.040
Benzene	2.27	1.500	330	459	8517	26044.76	0.002	0.003	0.339	0.039
DOX	2.25	1.422	325	460	9030	26254.18	0.024	0.030	0.302	0.040

The emission profile of MTCE demonstrates an approximately 60 nm red shift with increasing solvent polarity, as illustrated in **Figure 4b**. This shift is notably larger than observed in the absorption spectra, providing a clear indication that long-range electrostatic interactions play

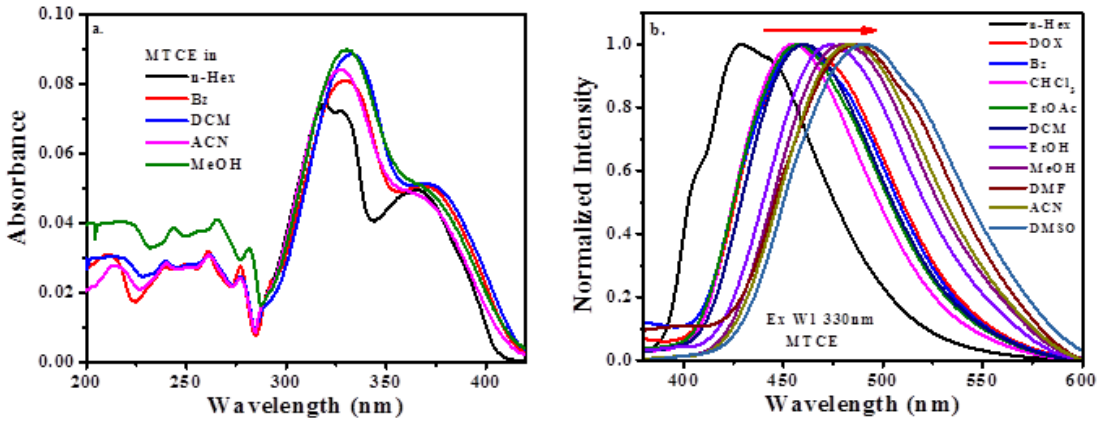

Figure 4. a. absorption spectra of MTCE (2 μM) in n-hexane (n-Hex),benzene (Bz), acetonitrile (CH_3CN), methanol (MeOH) and 1,2-dichloromethane (DCM). **b**. Normalized emission spectra of MTCE (2 μM) in n-hexane (n-Hex), 1,4-dioxane (DOX), benzene, chloroform ($CHCl_3$), ethylacetate (EtOAc), 1,2-dichloromethane, ethanol (EtOH), methanol, N, N-dimethylformamide (DMF), acetonitrile, dimethylsulfoxide (DMSO).

crucial role in stabilizing the more polar excited state to a greater extent than the ground state.[38] The electron-donating nature of the thiophene nucleus induces a displacement of π-electrons towards the coumarin nucleus, leading to a redistribution of π-electrons that enhances charge separation in the excited state. Dipole-dipole interactions between MTCE and polar solvents, along with dipole-induced dipole interactions with less polar solvents, contribute to a more substantial stabilization of the excited state compared to the ground state, which is stabilized by H-bond interactions.[39] Consequently, the overall energy difference between the ground and excited states decreases, resulting in the observed redshift in the emission profile. The μ_e value calculated from Lippert's equation was found to be larger than the values obtained from the other two equations, likely due to specific solute-solvent interactions.[18] The excited state of MTCE exhibits differently distributed charges compared to the ground state, leading to a large Stokes shift and thus a higher μ_e value (**Table 2**).

Table 2. Onsagar cavity radius and dipole moment data of MTCE

Molecular volume $(\frac{4}{3}\pi a^3)$ (˚A^3)	**Radius** ***(a)*** **(˚A)**	***m*** **(cm^{-1})**	***m*$_1$** **(cm^{-1})**	***m*$_2$** **(cm^{-1})**	μ_g **(D)**	μ_e **(D)**	$(\mu_e - \mu_g)$ **(D)**	$\frac{\mu_e}{\mu_g}$
221.238	3.751	8401.209	2465.865	3426.629	0.7	4.4	3.7	6.3

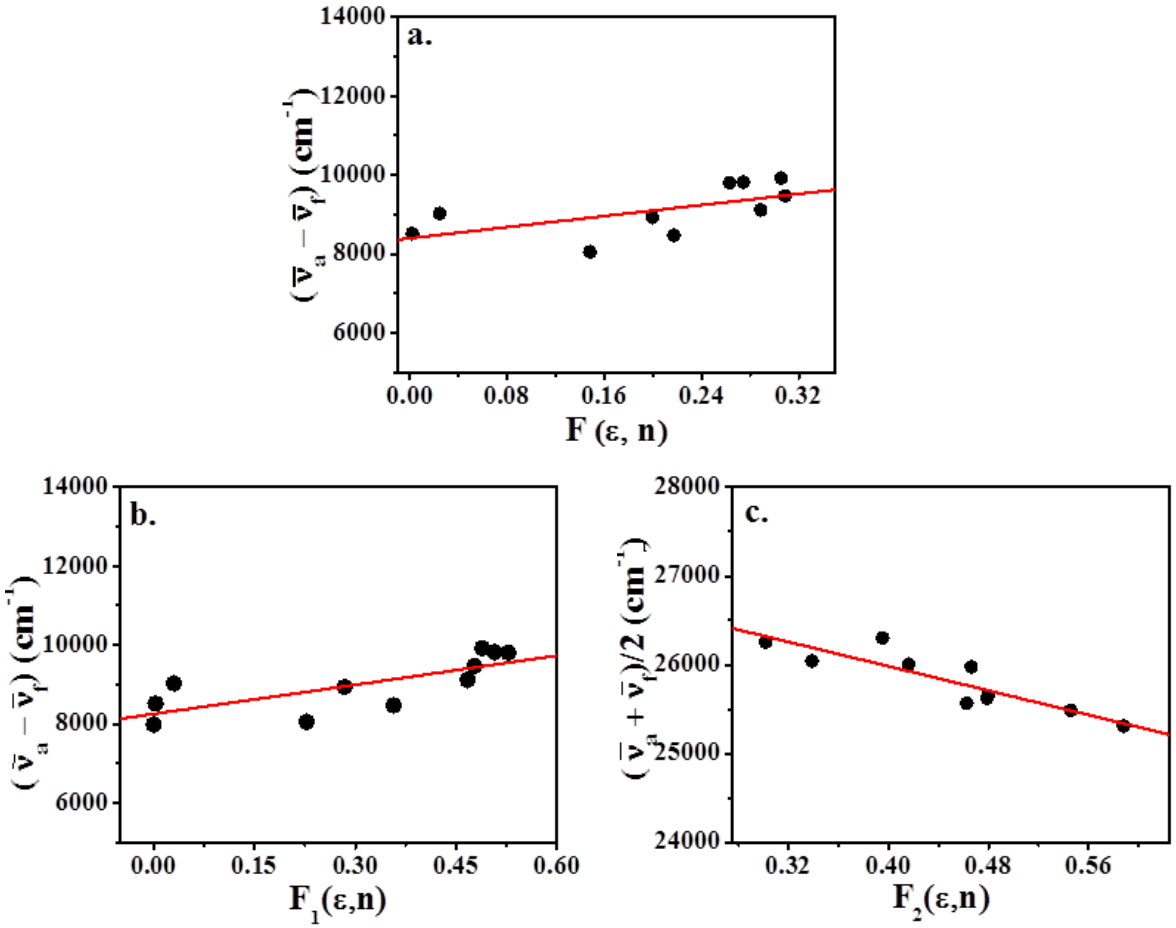

Figure 5. a. Lippert's plot. **b.** Bakhshiev's plot. **c.** Bilot-Kawski plot of MTCE (2 μM) in 1,4-dioxane (DOX), benzene, chloroform ($CHCl_3$), ethylacetate (EtOAc), 1,2-dichloromethane, ethanol (EtOH), methanol, N, N-dimethylformamide (DMF), acetonitrile, dimethylsulfoxide (DMSO).

Chapter IC: Fluorescence studies on the interaction of MTCE with BSA protein

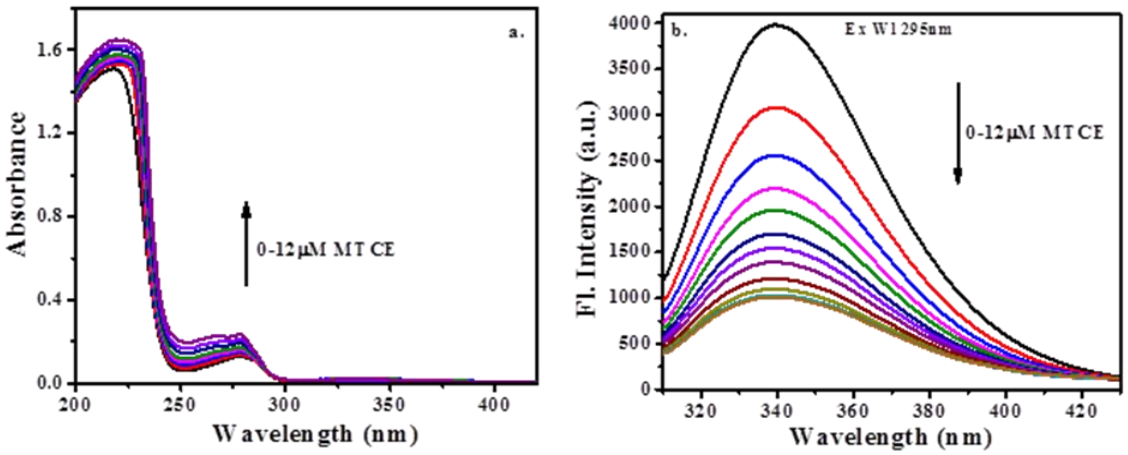

Figure 6. a. Absorbance spectra BSA-MTCE system. b. emission spectra at 293K of BSA-MTCE system with varying MTCE concentration (1-12μM) and fixed BSA concentration (3μM).

Having examined the medicinal attributes of angelicin, our focus shifted towards a comprehensive exploration of the interaction between the synthesized MTCE and BSA, utilizing fluorescence as the primary investigative tool. **Figure 6b** vividly illustrates the progressive quenching of the tryptophan emission band at 340 nm in BSA, underlining the impact of MTCE, particularly evident when the excitation wavelength was consistently set at 295 nm. The F_0/F vs [MTCE] plot in **Figure 7a**. showed good linearity at each of the three temperatures at 293 K, 300 K, and 310 K, indicating a single quenching process occurred. The decrease of Stern-Volmer constant, K_{SV} with increasing temperature, indicating a static quenching mechanism, was attributed to the formation of a non-fluorescent BSA-MTCE complex (**Table 3**). The bimolecular quenching constant, k_q, calculated in the order of 10^{13} $Lmol^{-1}s^{-1}$, was much larger than the diffusion-controlled quenching constant limit, 2.0×10^{10} $Lmol^{-1}s^{-1}$, and the value also decreased with increasing temperature.[40] To confirm the static quenching mechanism, we analyzed the fluorescence quenching data using the modified Stern-Volmer equation or the double reciprocal equation. The good linear relationship shown in **Figure 7b** indicates that a single mechanism is responsible for the quenching observed in the study. The Stern-Volmer constant of the accessible fluorophore, K_a, decreases with increasing temperature. The corresponding values are listed in **Table 4**. Additionally, the fraction of

accessible fluorophore, f_a, falls from 0.909 to 0.857. The observed changes are clear indications of the complex's instability at higher temperatures, suggesting a static quenching mechanism due to the formation of a non-fluorescent BSA-MTCE complex.[41]

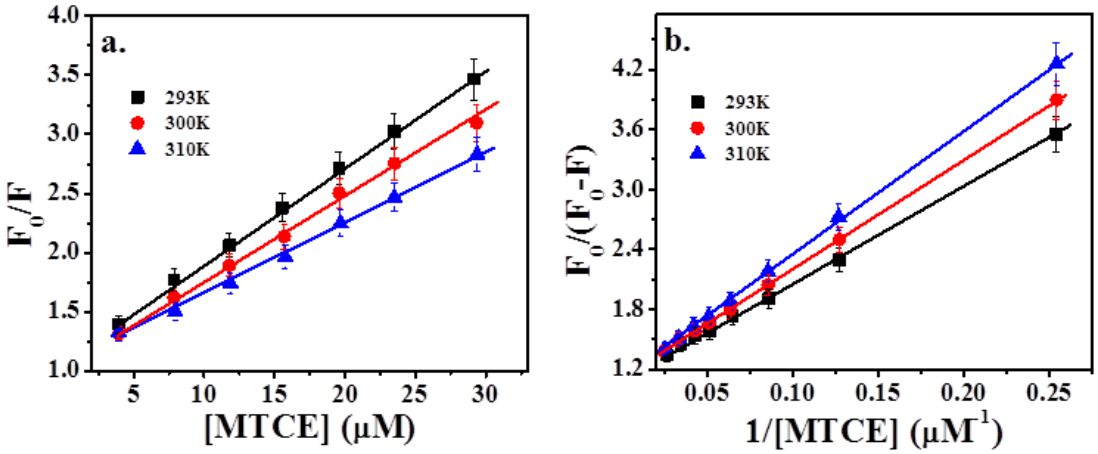

Figure 7. a. Stern-Volmer plot. **b.** Modified Stern-Volmer plot

We also measured the UV-vis absorption spectra of the BSA-MTCE system to support the quenching mechanism. The change in the UV-Vis absorption spectra in **Figure 6a** at ~210 nm with a red shift and ~280 nm with a blue shift was due to the alteration of protein conformation by forming a ground-state complex between BSA and MTCE.

Table. 3 Bimolecular quenching rate constants, Stern-Volmer constants, modified Stern-Volmer constants and fraction of accessible fluorophore for BSA-MTCE complex

Temperature (*K*)	***Kq* ($M^{-1}s^{-1}$) X 10^{13}**	***KSV* (M^{-1}) X 10^4**	***R²***	***Ka* (M^{-1}) X 10^4**	***fa***	***R²***
293	1.734	8.670 ± 0.113	0.967	11.462 ± 0.097	0.909	0.967
300	1.503	7.367 ± 0.092	0.989	10.140 ± 0.040	0.894	0.989
310	1.252	6.261 ± 0.072	0.929	8.826 ± 0.108	0.857	0.929

To gain further insight into the complexation process, we calculated the binding constant (K_b) and number of binding sites (n) using the well-known double logarithmic equation [40] by analyzing the fluorescence data at three different temperatures.

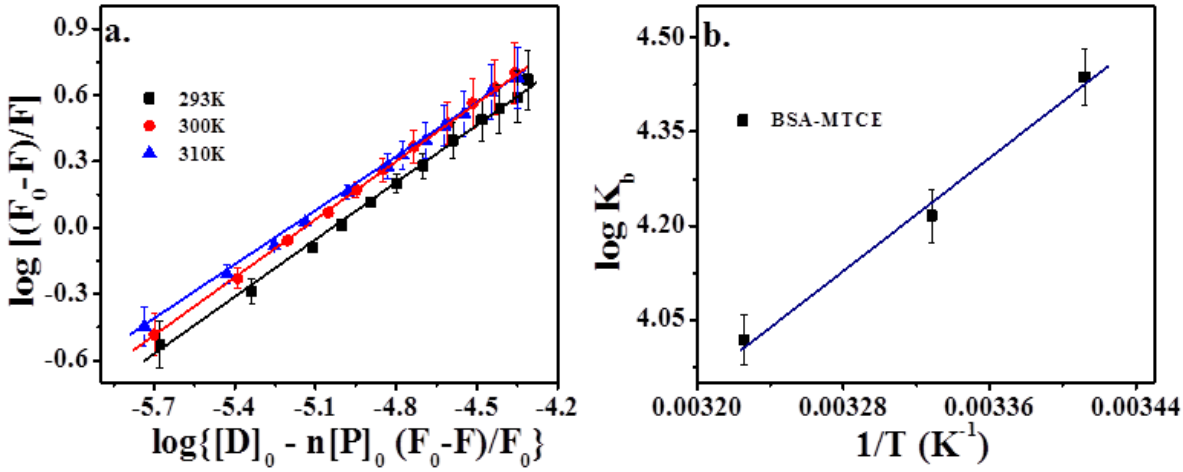

Figure 8. a. Double logarithm plot. **b.** van't-Hoff plot.

In **Table 4,** the negative ΔG values indicate the spontaneity of the complexation process. Moreover, |ΔH| > |TΔS| also indicates an entropy-driven complexation process occurred in the BSA-MTCE system. The ΔG values with increasing temperatures also support the idea that the complexation becomes destabilized at high temperatures. The values of the number of binding sites (n) at the experimental temperatures are approximately equal to 1, indicating that there is one type of binding site for MTCE with BSA and the tryptophan is near or within the binding site. In BSA, the tryptophan residues involved in binding can be either Trp-134 or Trp-213, with Trp-134 being more exposed to a hydrophilic environment, whereas Trp-213 is deeply buried in the hydrophobic loop.[25]

Table 4. Binding constant and thermodynamic parameters of BSA-MTCE system

T (K)	$logK_b$	*n*	R^2	K_b (M^{-1})	Δ*G* (kJmol^{-1})	Δ*S* (Jmol^{-1})	Δ*H* (kJmol^{-1})
293	4.437 ± 0.072	0.880 ± 0.015	0.945	2.736×10^4	-24.892	-61.067	-42.730
300	4.216 ± 0.024	0.891 ± 0.005	0.998	1.646×10^4	-24.220		
310	4.019 ± 0.034	0.823 ± 0.007	0.926	1.045×10^4	-23.855		

Chapter ID: Fluorescence studies on the Interaction of MTCE with metal ions

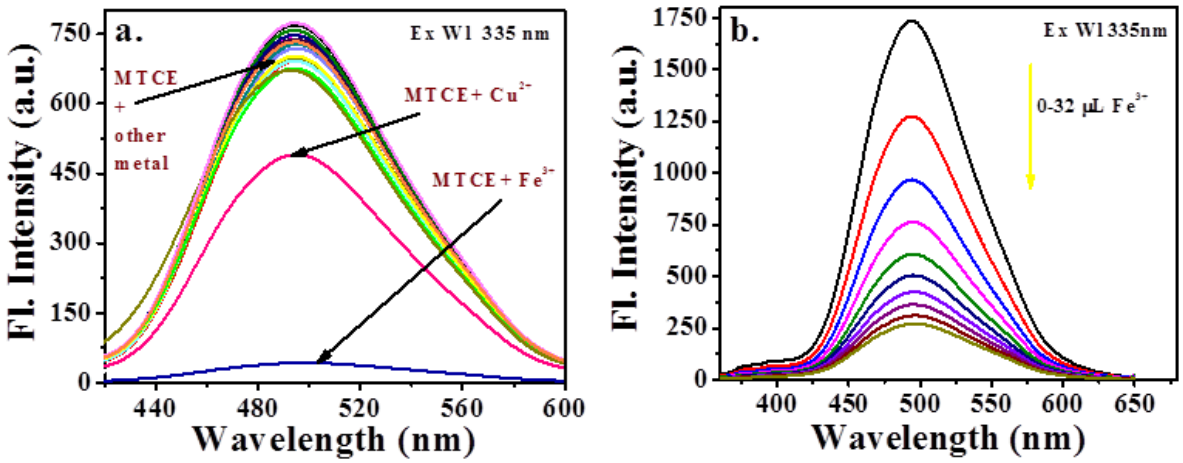

Figure 9. a. Emission spectra of MTCE (5 µM) in presence of equivalent amount (10µM) of different metal ions (Na^+, K^+, Mg^{2+}, Ca^{2+}, Ba^{2+}, Al^{3+}, Fe^{3+}, Co^{2+}, Ni^{2+}, Cu^{2+}, Zn^{2+}, As^{3+}, Pb^{2+}, Hg^{2+}, Cd^{2+}) **b.** Emission titration spectra of MTCE (10 µM) in water/ethanol (1:1, v/v; 0.01 M tris-HCl; pH : 7.4) with varying concentration of Fe^{3+} ion (3-32 µM).

We investigated the sensing behavior of MTCE in the presence of different common metal ions in water/ethanol (1:1, v/v; 0.01M tris-HCl; pH: 7.4) using the fluorescence method. In **Figure 9a**, the emission band of MTCE at 495 nm exhibited an immediate 'turn off' fluorescence with the addition of Fe^{3+} over the equivalent amount (10µM) of other metal ions (Na^+, K^+, Mg^{2+}, Ca^{2+}, Ba^{2+}, Al^{3+}, Co^{2+}, Ni^{2+}, Cu^{2+}, Zn^{2+}, As^{3+}, Pb^{2+}, Hg^{2+}, Cd^{2+}). The fluorescence intensity was quenched by about 80%, which may be due to the ligand-to-metal charge transfer (LMCT) mechanism.[45] The unfilled 'd' orbital of the paramagnetic Fe^{3+} may participate in the electron transfer from MTCE, leading to fluorescence quenching by opening a non-radiative deactivation channel.[46] To obtain more perceptivity, we investigated the fluorescence titration of MTCE by gradually adding Fe^{3+} (**Figure 9b**). The Stern-Volmer plot showed linearity up to 8.5 µM, but above that concentration, it displayed a nonlinear upward curvature due to the poor accessibility of the quencher in the vicinity of the sphere around MTCE (Figure 10a). The Stern-Volmer constant ($K_{sv'}$) at 298K was calculated to be 4.84 x 10^4 M^{-1} (R^2 = 0.9968).In Figure 10b, the modified Stern-Volmer plot exhibits excellent linearity, and the Stern-Volmer constant $K_{sv''}$ for accessible fluorophores is calculated to be 2.57 × 10^4 M^{-1}, indicating a strong quenching effect. Additionally, it is noteworthy that almost 92% of the

fluorophores are accessible for quenching, suggesting the high sensitivity of MTCE towards Fe^{3+} ions.

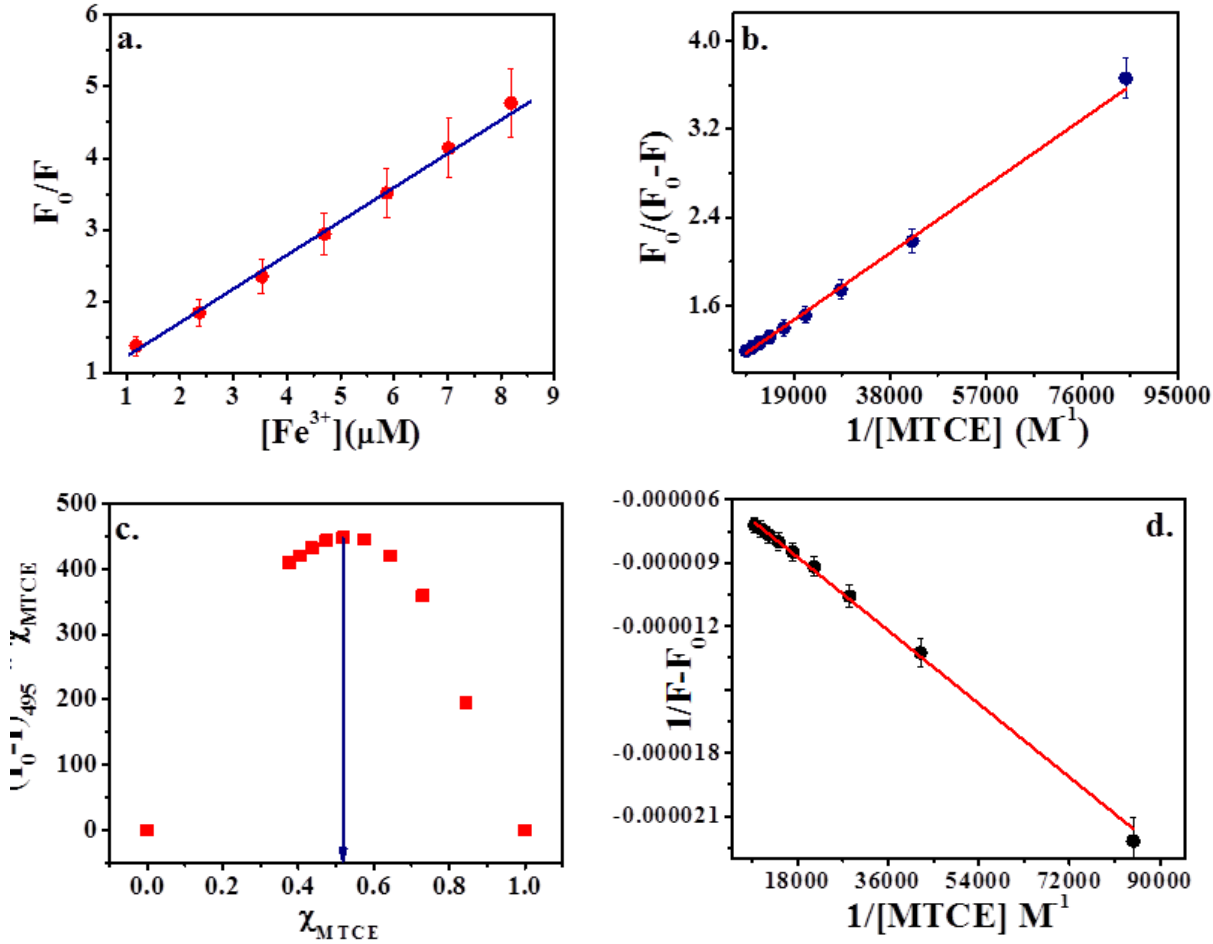

Figure 10. a. Stern-Volmer plot **b.** modified Stern-Volmer plot **c.** Job's plot **d.** B-H plot of MTCE and Fe^{3+} in water/ethanol (1:1, v/v; 0.01M tris-HCl; pH: 7.4) at 335 nm excitation wavelength.

The Job's plot displays a maximum at a molar fraction of approximately 0.52, indicating the formation of a 1:1 stoichiometry complex, and the wide curvature implies an evenly distributed equilibrium in the MTCE-[Fe^{3+}] system (**Figure 10c**).[47] The association constant (K_a') was determined to be 3.03×10^4 M^{-1} (R^2 = 0.9985) using the Benesi-Hildebrand method (**Figure 10d**).[48] The negative value of ΔG (-25.57 kJmol^{-1} at 298K) supports the spontaneity of the complexation process. To assess the practical applicability of MTCE as a selective Fe^{3+} sensor, a competitive experiment was conducted in the presence of Fe^{3+} mixed with equivalent amounts of other metal ions (**Figure 11**). Interestingly, in every case, the fluorescence emission intensity was quenched immediately after the addition of Fe^{3+} to each of the candidate metal

ions. Therefore, MTCE or its analogue appears to be a very promising candidate for the detection of Fe^{3+}.

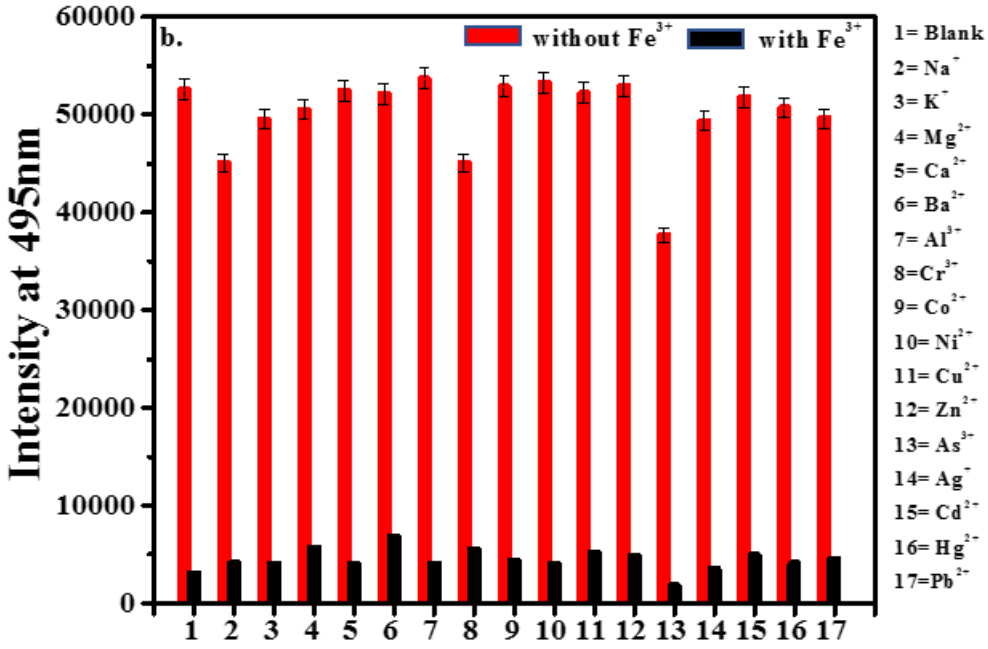

Figure 11. Bar diagram of selectivity profile of Fe^{3+} toward MTCE.

Chapter IE: Fluorescence studies on the interaction of MTCE with β-Cyclodextrin

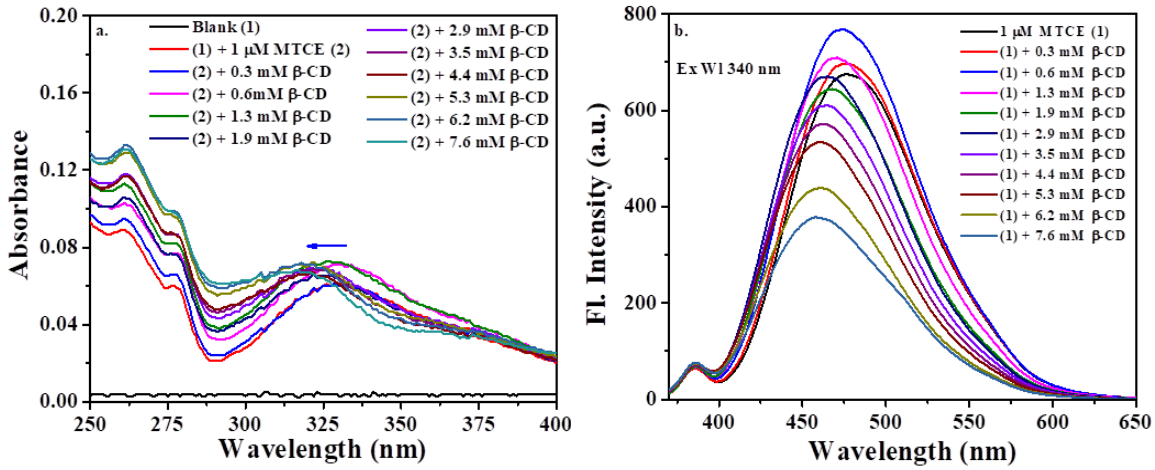
a.
Blank (1)
(1) + 1 μM MTCE (2)
(2) + 0.3 mM β-CD
(2) + 0.6mM β-CD
(2) + 1.3 mM β-CD
(2) + 1.9 mM β-CD
(2) + 2.9 mM β-CD
(2) + 3.5 mM β-CD
(2) + 4.4 mM β-CD
(2) + 5.3 mM β-CD
(2) + 6.2 mM β-CD
(2) + 7.6 mM β-CD
Absorbance
Wavelength (nm)
b.
Ex Wl 340 nm
1 μM MTCE (1)
(1) + 0.3 mM β-CD
(1) + 0.6 mM β-CD
(1) + 1.3 mM β-CD
(1) + 1.9 mM β-CD
(1) + 2.9 mM β-CD
(1) + 3.5 mM β-CD
(1) + 4.4 mM β-CD
(1) + 5.3 mM β-CD
(1) + 6.2 mM β-CD
(1) + 7.6 mM β-CD
Fl. Intensity (a.u.)
Wavelength (nm)

Figure 12. a. Absorbance spectra and b. emission spectra at 293K of β-CD_MTCE system with varying β-CD concentration (0.0-7.6 mM) and fixed MTCE concentration (1 μM).

In this Chapter, our focus has been centered on exploring the interplay between thieno-angelicin derivative, MTCE, and β-cyclodextrin. The energetically minimized structure of MTCE revealed a diameter of 7.4 Å,[49] a dimension notably comparable to that of β-cyclodextrin. Motivated by this congruence, our investigation delved into the potential formation of an inclusion complex between β-cyclodextrin and MTCE, employing fluorescence studies. The anticipated outcome of such a complex formation is expected to exert a profound influence on the reactivity, as well as the spectroscopic and electrochemical characteristics of the guest molecule. To unravel the intricacies of this interaction, UV-absorption and fluorescence studies were meticulously conducted across varying temperatures and subsequently, thermodynamic parameters were calculated to further elucidate the nuances of the system.

In **Figure 12** both absorption and emission spectra of 1 μM MTCE in tris-HCl buffer of pH 7.4 has displayed with varying concentration of β-cyclodextrin (0.0-7.6 mM). We maintain the physiological condition by keeping the medicinal properties of Angelicin. With increasing the β-CD concentration the main absorption peak has shifted from 340 nm to 320 nm with diminishing the 370 nm hump and also the emission intensity decreases. These may be due to the formation of non-emissive inclusion complex at the ground state. The linearity in the

Benesi-Hildebrand plot (**Figure 13a**) also suggest an 1:1 β-CD_MTCE inclusion complex formation. The Inclusion or association complex (K_a) at three different temperature were evaluated from the slope of the B-H plot.

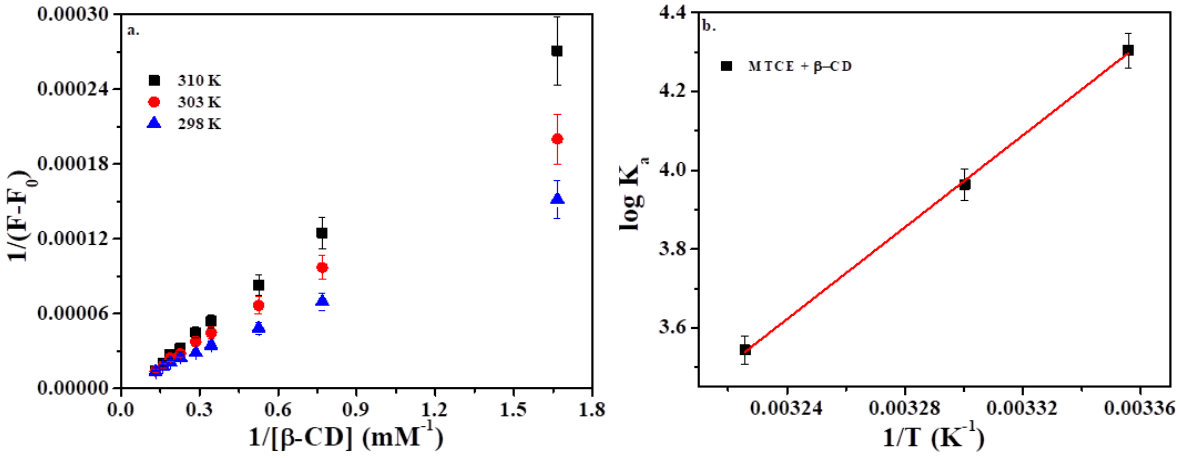

Figure 13. a. Benesi-Hildebrand plot. and **b.** van't-Hoff plot. of β-CD_MTCE system at 298K, 303K and 310K.

The thermodynamic parameters, ΔH and ΔS were calculated as -111.67 kJ mol^{-1} and -292.38 $Jmol^{-1}$ from the slope and intercept of the vant Hoff plot (**Figure 13b**) respectively. ΔG was then calculated at three different temperatures as summarized in **Table 5**. The negative ΔG values indicate the spontaneity of the inclusion process. Moreover, |ΔH| > |TΔS| also indicates an enthalpy-driven complexation process occurred in the b-CD_MTCE system. The ΔG values with increasing temperatures also support the idea that the complexation becomes destabilized at high temperatures.

Table 5. Association constant and thermodynamic parameters of β-CD_MTCE system at 298K, 303K and 310K.

T (K)	***logKa***	***R²***	***Ka* (M^{-1})**	**Δ*G* ($kJmol^{-1}$)**	**Δ*S* ($Jmol^{-1}$)**	**Δ*H* ($kJmol^{-1}$)**
298	4.403 ± 0.098	0.995	20.1×10^3	-24.89	-292.38	-111.67
303	3.964 ± 0.090	0.998	9.2×10^3	-24.22		
310	3.544 ± 0.094	0.996	3.5×10^3	-23.856		

Conclusion

In summary, we have developed an efficient and high-yielding total synthesis of a novel derivative of thienoangelicin, MTCE, from suitable β-chloro-α,β-unsaturated aldehyde. Our investigations into the interaction of MTCE with BSA, solvents, and metal ions using fluorescence studies suggest that MTCE is a promising candidate for therapeutic studies, optical sensing, and fluorescence probing. We found that the ground state of MTCE is stabilized by intermolecular H-bonding interactions with solvents, whereas the more polar excited state is more stabilized with increasing solvent polarity due to long-range electrostatic interactions. The theoretically calculated ground and excited state dipole moments of MTCE are well-correlated with the experimentally calculated values. MTCE interacts with BSA in subdomain IIA by forming a non-fluorescence complex. The calculated binding and thermodynamic parameters have justified the involvement of hydrogen bonding and van der Waal forces in the binding interaction in the complexation process. Interestingly, MTCE also exhibits a selective sensing property towards Fe^{3+} in a semi-aqueous medium, with a lowest detection limit of 0.35 μM.

References

[1] C. K. Mahendra, L.T. H. Tan, W. L. Lee, W. H. Yap, P. Pusparajah, L. E. Low, S.Y. Tang, K. G. Chan, L. H. Lee, B. H. Goh, *Frontiers in Pharmacology.*, **2020**, *11*, 366.

[2] M. Lenković, L. Cabrijan, F. Gruber, M. Saftić, Z. StanićZgombić, A. Stasić, V. Peharda, *Collegium Antropologicum*., **2008**, *32 (2)*, 203.

[3] E. L. Grant, R. C. Von Borstel, M. J. Ashwood-Smith, *Environ. Mol. Mutagen*., **1979**, *1 (1)*, 55.

[4] P. C. Joshi, M. A. Pathak, *Biochem. Biophys. Res. Commun*., **1983**, *112 (2)*, 638.

[5] I. Lampronti, N. Bianchi, M. Borgatti, E. Fibach, E. Prus, R. Gambari, *Eur. J. Haematol.*, **2003**, *71 (3)*, 189.

[6] H. J. Cho, S. G. Jeong, J. E. Park, J. A. Han, H. R. Kang, D. Lee, *Antiviral Res.*, **2013**, *100 (1)*, 75.

[7] F. Liu, G. Q. Sun, H. Y. Gao, R. S. Li, L. W. Soromou, N. Chen, Y. H. Deng, H. H. Feng, *J. Surg. Res*., **2013**, *185 (1)*, 300.

[8] F. Wang, J. Li, R. Li, G. Pan, M. Bai, Q. Huang, *Mol. Med. Rep*., **2017**, *16 (4)*, 5441.

[9] X. Li, C. Yu, Y. Hu, X. Xia, Y. Liao, J. Zhang, H. Chen, W. Lu, W. Zhou, Z. Song, *Front. Cell. Infect. Microbiol*., **2018**, *8*, 178.

[10] F. Bordin, F. Baccichetti, F. Carlassare, *Naturforsch.*, **1978,** *33*, 296.

[11] R. Aneja, S. K. Mukerjee, T. R. Seshadri, *Tetrahedron*, **1958**, *2*, 203.

[12] M. Luisa, L. P. Eleonora, M. Giulia, M. Christine, B. Francarosa, F. Giuseppe, F. Walter, P. Brunella, *Farmaco*, **1998**, *53*, 602.

[13] S. Francisco, L. R. Rodrigues, N. Cerqueira, A. Oliveira-Campos, A. Esteves, *European Journal of Medicinal Chemistry*, **2014,** *87*, 298.

[14] S. Joshi, S. Kumari, R. Bhattacharjee, A. Sarmah, R. Sakhuja, D. D. Pant, *Sensors and Actuators B.*, **2015,** *220*, 1266.

[15] D. Nagaraja, N. R. Patil, R. A. Kusanur, H. D. Patil, R. M. Melavanki, *Internationa Journal of Life science and Pharma Research*, **2013**, *3(1)*, 54.

[16] S. Chandrasekhar, H.R. Deepaa, R.M. Melavanki, S. Mogurampelly, M. M. Basanagouda, S. Yallappa, J. Thipperudrappa, *Chemical Data Collections*, **2020,** *29*, 100516.

[17] M. M. Chebli, S. M. Hamdi, A. Rabahi, A. M. S. Silva, M. Hamdi, *Journal of Molecular liquids*, **2013**, *181*, 89.

[18] E. Z. Lippert., *Naturforsch*, **1955**, 541.

[19] N.G. Bakshiev, *Opt. Spektrosk*., **1964**, *16*, 821.

[20] L. Bilot, A. Z. Kawski, *Naturforsch*., **1962**, *17a*, 621.

[21] L. Bilot, A. Z. Kawski, *Naturforsch*., **1963,** *18a*, 256.

[22] T. Jiang, K. Zhou, Y. Lou, D. Pan, J. Shi, *J. Biomol. Struct. Dyn*., **2018,** *36*, 1095.

[23] Y. Wang, Y. Wang, Q. Luo, H. Zhang, J. Cao, *Spectrochim. Acta Part A*, **2019,** *206*, 538.

[24] Y. Ni, R. Zhu, S. Kokot, *Analyst 136*, **2011**, *22*, 4794.

[25] S. Chatterjee, T. K. Mukherjee, *Phys. Chem. Chem. Phys*., **2014**, *16*, 8400.

[26] A. Roy, P. Seal, J. Sikdar, S. Banerjee, R. Haldar, *J. Biomol. Struct. Dyn.*, **2018,** *36*, 387.

[27] D. C. Carter, J. X. Ho, *Adv. Protein Chem*., **1994**, *45*, 153.

[28] K. Sakai-Kato, M. Kato, H. Nakakuki, T. Toyóoka, *J. Pharmaceut. Biomed*., **2009**, *31*, 299.

[29] K. P. Carter, A. M. Young, A. E. Palmer, *Chemical Reviews*, **2014**, *114*, 4564.

[30] Y. Yang, Q. Zhao, W. Feng, F. Li, *Chemical Reviews*, **2013**, *113*, 192.

[31] D. Cao, Z. Liu, P. Verwilst, S. Koo, P. Jangjili, J. S. Kim, W. Lin, *Chemical Reviews*, **2019**, *119 (18)*,10403.

[32] X. Sun, T. Liu, J. Sun, X. Wang, *RSC Advance*, **2020**, *10*, 10826.

[33] M. S. Norfatirah, C. Alexander, M. Stephen, M. Peter, G. S. Anna, A. Zanariah, A. T. Hairul, M. Simon , *Scientific Reports*, **2020**, *10*, 7421.

[34] P. Aisen, M. Wessling-Resnick, E. A. Leibold, *Curr. Opin. Chem. Biol.*, **1999**, *3*, 200.

[35] K. Samanta, G. K. Kar, A. K. Sarkar, *Tetrahedron Lett.*, **2008,** *49*,1461.

[36] T. B. Maiti, G. K. Kar, *Heterocycles*, **2009**, *78(12)*, 3073.

[37] N. P. Buu-Hoi, N. Hoan, N. H Khoi, *Recl. Trav. Chim. Pays-Bas*, **1950**, *69*, 1053.

[38] N. A. Murugan, H.W. Hugosson, H. Agren, *J. Phys. Chem. B.,* **2008**, *112*, 14673.

[39] B. Siddlingeshwar, S. M. Hanagodimath, E.M. Kirilova, G. K. Kirilov, *J. Quant. Spectrosc. Radiat. Transfer*., **2011**, *112*, 448.

[40] S.-B. Kou, Z.-Y. Lin, B.-L. Wang, J.-H. Shi, Y.-X. Liu, *Journal of Molecular Structure*, **2020**, *1224*, 129024.

[44] B. -L. Wang, S. -B. Kou, Z. -Y. Lin, J. -H. Shi, Y. -X. Liu, *International Journal of Biological Macromolecules*, **2020**, *157*, 340.

[45] M. S. Norfatirah, C. Alexander, M. Stephen, M. Peter, G. S. Anna, A. Zanariah, A. T. Hairul, M. Simon , *Scientific Reports*, **2020**, *10*, 7421.

[46] L. Yang, W. Yang, D. Xu, Z. Zhang, A. Liu, *Dyes and Pigments*., **2013**, *97*, 168.

[47] J. S. Renny, L. L. Tomasevich, E. H. Tallmadge, D. B. Collum, *Angew Chem Int Ed Engl.*, **2013,** *46*, 11998.

[48] H. A. Benesi, J. H. Hildebrand, *J. Am. Chem. Soc*., **1949**, *71*, 2703.

[49] T. Biswas, I. Haque, S. Roy, B. Chakraborty, D. Mitra, G. K. Kar, A. Halder, ChemistrySelect, **2023,** *8*, e202300857.

Chapter II: Thiophene analogue of stilbene derivative: (*E*)-1,2-bis(7-methylbenzo[1,2-b:3,4-b']dithiophen-2-yl)ethene (MTS)

Introduction

The study of condensed thiophene derivatives has assumed distinctive significance within the realm of synthetic organic chemistry**.** Bioisosteric relationships exist between -CH=CH- and 'S' (referred to as ring equivalents), leading to greater similarities in both physical and chemical properties between the thiophene and benzene rings.[1] The identification of polyaromatic thiophene derivatives in coal tar and shale oil has notably captured the interest of synthetic chemists. Consequently, a substantial number of syntheses of polycyclic thiaarenes (PTA) have emerged over the last few decades, reflecting the increased focus on this intriguing class of compounds.[2-7] Condensed thiophenes with extended conjugation demonstrate the capacity to operate as p-type conducting molecules in Organic Thin Film Transistors (OTFTs), as well as in Organic Photovoltaics and Dye-Sensitized Solar Cells.[8-11] Helicenes represent a captivating category of chiral helical molecules composed of ortho-fused aromatic rings, showcasing numerous intriguing features and the ability to function as organic conductors.[12-15] Thia[n]helicenes, a subclass of heterohelicenes where benzene rings alternate with thiophene rings, have garnered significant attention owing to their distinctive characteristics that blend the electronic properties of oligothiophenes with the unique chiroptical features associated with the helical structure for the applications in nonlinear optics, organic electronic devices, catalysis, electrochemical sensing, biology.[14,16-24]

In this chapter, we concentrate on the synthesis of a thiophene analogue of stilbene derivative, specifically (*E*)-1,2-bis(7-methylbenzo[1,2-b:3,4-b']dithiophen-2-yl)ethene (**10**), which serves as a precursor to tetrathiahelicene. The synthesis has been achieved *via* McMurry coupling of 7-methylbenzo[1,2-b:3,4-b']dithiophene-2-carbaldehyde (**9**). The incorporation of the second thiophene ring is accomplished through the base-catalyzed condensation of methyl thioglycolate with 4-chloro-2-methyl-6,7-dihydrobenzo[b]thiophene-5-carbaldehyde (**1**).

Chapter IIA: Synthesis of MTS

The retrosynthesis of thiophene analogue of stilbene derivative (*E*)-1,2-bis(7-methylbenzo[1,2-b:3,4-b']dithiophen-2-yl)ethene (**10**) has been depicteted in **Figure 1**. The target molecules can be synthesized starting from 4-chloro-2-methyl-6,7-dihydrobenzo[b]thiophene-5-carbaldehyde (**1**) which was obtained from 2-methyl-6,7-dihydrobenzo[b]thiophen-4(5H)-one *via* Vilsmeier-Haack reaction as stated in the **Chapter IA (Synthesis of MTCE)**.

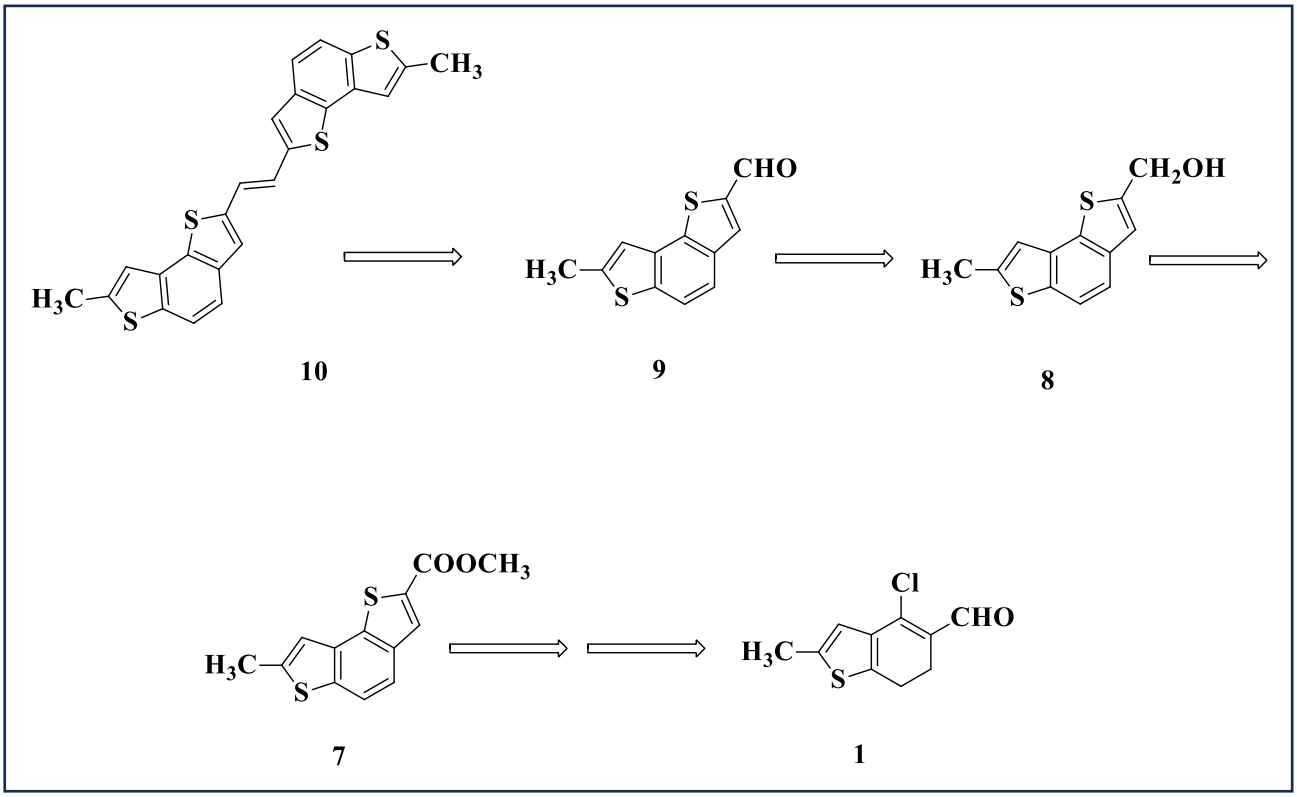

Figure 1. Retrosynthesis of the thiophene analogue of stilbene derivative **10** (MTS).

The synthesis of (*E*)-1,2-bis(7-methylbenzo[1,2-b:3,4-b']dithiophen-2-yl)ethene (**10**) has been presented in **Figure 2**. The *β*-chloro-*α,β*-unsaturated aldehyde (**1**) when subjected to condensation with methyl thioglycolate underwent an addition elimination reaction followed by aldol type condensation to produce the dihydro bisthiophene derivative **6** in 74.5 % yield. The structure of the compound **6** was confirmed by ^{1}H-NMR (400 MHz, $CDCl_3$) data (**Figure 3**) and HRMS data (ESI, 70 eV): m/z $[M+H]^+$ calculated for $C_{13}H_{13}O_2S_2$: 265.0359; found: 265.0356. The ester derivative **6** was then aromatized with DDQ in refluxing benzene and the aromatized product methyl 7-methylbenzo[1,2-b:3,4-b']dithiophene-2-carboxylate **(7)** was obtained as a pale yellow solid in 98 % yield. **Figure 3.** as well as HRMS data (ESI, 70 eV): m/z $[M+H]^+$ calculated for $C_{13}H_{11}O_2S_2$: 263.0202; found: 263.0200 supported the structure.

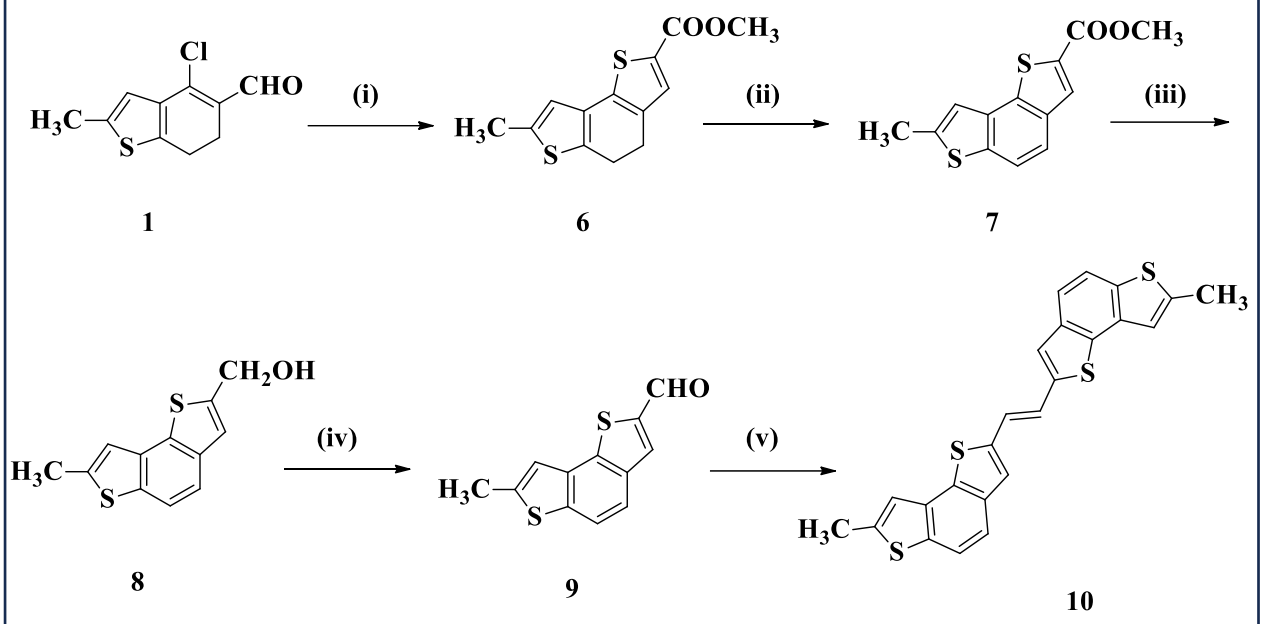

(i) HS-CH_2-$COOCH_3$, pyridine, Et_3N, 0-60 ˚C, 2hrs, then 50% KOH, 0 ˚C, 30 min (74.5%); (ii) DDQ, benzene, reflux, 2 hrs, (98%); (iii) $LiAlH_4$, dry ether, r.t, (89%); (iv) CrO_3, pyridine, 0-15 ˚C, (79%); (v) Zn, $TiCl_4$, DME, reflux, 4 hrs, (70%).

Figure 2. Synthesis of thiophene analogue of stilbene derivative (E)-1,2-bis(7-methylbenzo[1,2-b:3,4-b']dithiophen-2-yl)ethene (MTS)

The compound **7** on $LiAlH_4$ reduction furnished the alcohol derivative **8** with 89 % yield. In ^{1}H-NMR data appearance of the signals respectively at δ 2.04 (br, 1H for OH proton) and 4.95 (s, 2H for CH_2 proton) along with disappearance of the singlet at δ 4.01 for methyl ester protons confirmed the successful conversion ester functionality into primary alcohol. The alcohol derivative (7-methylbenzo[1,2-b:3,4-b']dithiophen-2-yl)methanol (**8**) was then successfully converted in good yield to the aldehyde derivative **9** by oxidation with CrO_3 in dry pyridine. The proton signal at δ 10.11 (s, 1H) ppm in ^{1}H-NMR data indicated the conversion of primary alcohol to aldehyde. HRMS data also supported the structure of the compound **9**. HRMS (ESI, 70 eV): m/z $[M+H]^+$ calculated for $C_{13}H_{11}O_2S_2$: 233.010; found: 233.0094. The compound **9** (7-methylbenzo[1,2-b:3,4-b']dithiophene-2-carbaldehyde) was then subjected to McMurry coupling reaction ($TiCl_4$, Zn dust, DME, reflux, Argon atmosphere) to furnish the desired alkene **10** in 70% yield as a lemon yellow solid. The proposed structure of the alkene is in well

agreement with its ^{1}H-NMR data (**Figure 3).** All the compounds **6-9** are also supported by the ^{13}C-NMR data. However, due to very poor solubility of compound **10** in $CDCl_3$ or DMSO-d_6 we could not record it ^{13}C-NMR data. Although HRMS data (ESI, 70 eV): m/z $[M+H]^+$ calculated for $C_{24}H_{17}S_4$: 433.0215; found: 433.0234 supported the structure of the compound **10**.

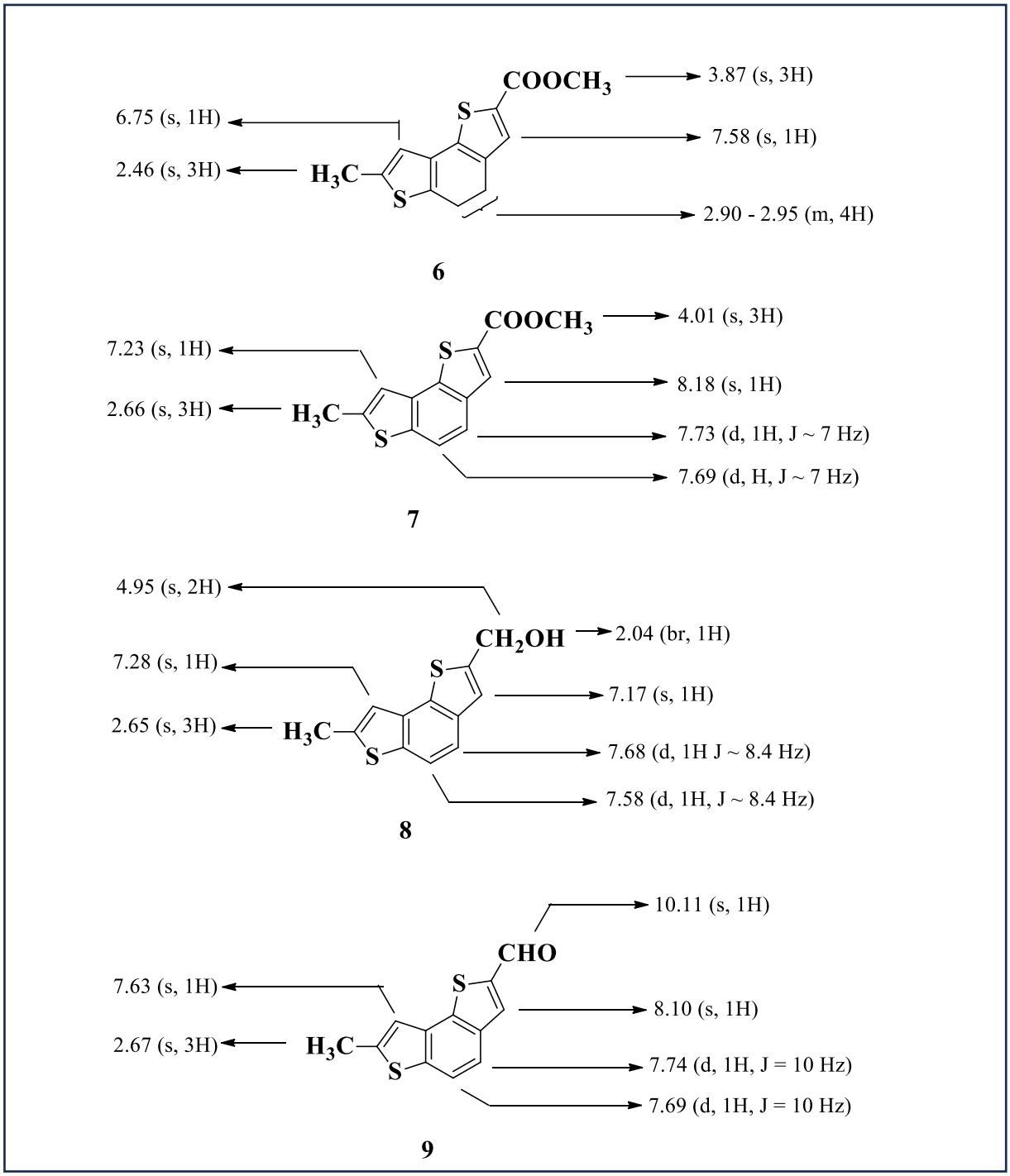

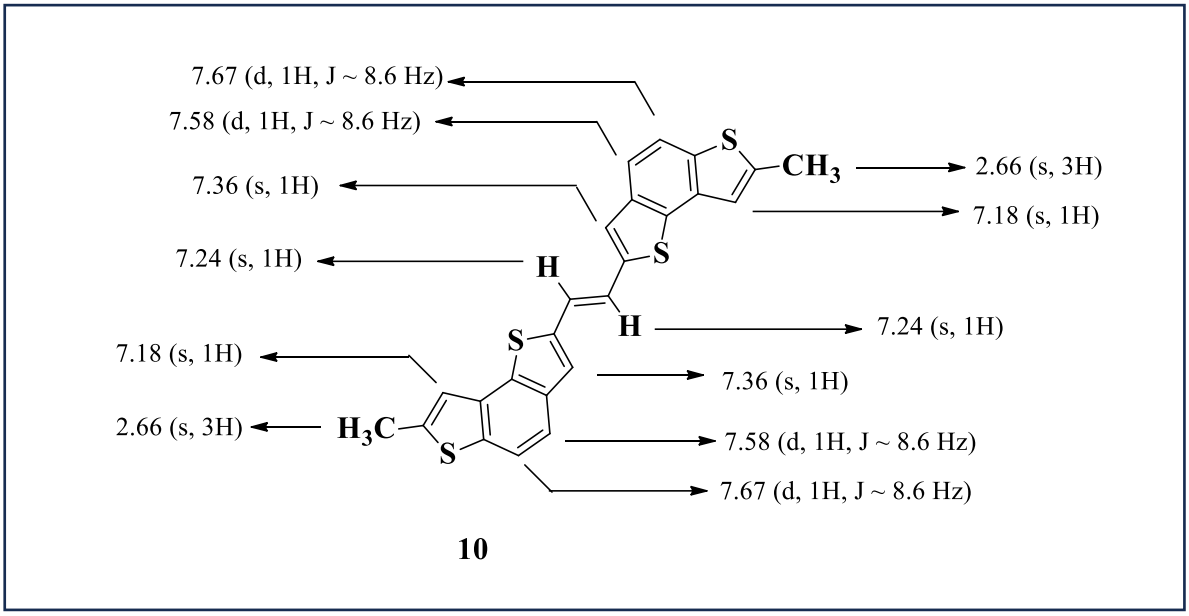

Figure 3. Tentative assignments of ^{1}H-NMR chemical shift (δ, ppm) and the splitting pattern of compound **6-10.**

Chapter IIB.

Fluorescence studies on the interaction of MTS with solvents

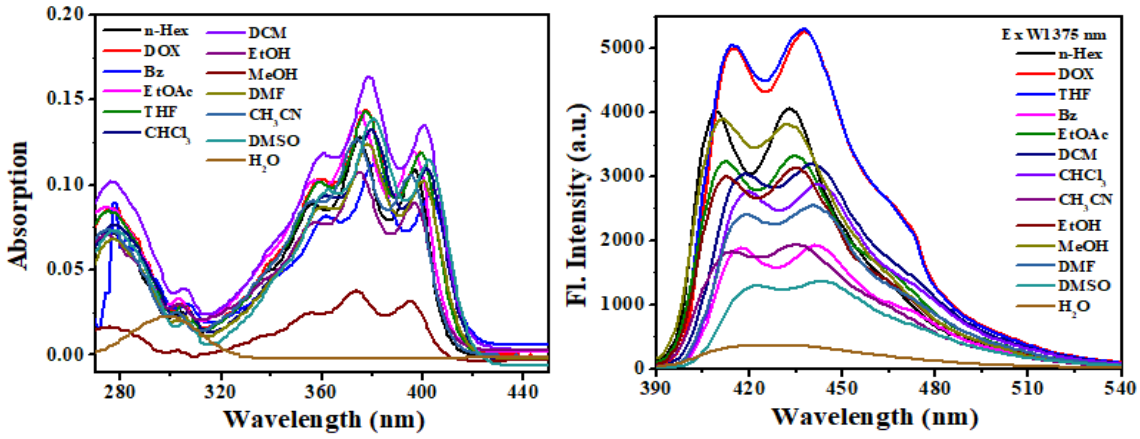

Figure 4. absorption spectra and emission spectra of MTS (2 μM) n-hexane (n-Hex), 1,4-dioxane (DOX), benzene (Bz), chloroform ($CHCl_3$), ethylacetate (EtOAc), Tetrahydrofuran (THF), 1,2-dichloromethane (DCM), ethanol (EtOH), methanol, N, N-dimethylformamide (DMF), acetonitrile (CH_3CN), dimethylsulfoxide (DMSO).

This chapter contain the detail studies of the synthesized theinostilbene derivative MTS and its fluorescence interaction with different solvents. The corresponding UV-absorption and

emission spectra have been displayed in **Figure 4** and the related spectral parameters have been tabulated in **Table 1.**

Table 1. Quantum yield, solvent parameter and spectral data of MTS in different solvents

Solvents	Dielectric constant	Refractive index	Quantum yield	Abs maxima	Emission max	Emission max
DMSO	46.7	1.48	0.32	380	422	443
DMF	36.7	1.43	0.54	378	419	441
CH_3CN	37.5	1.34	0.34	374	414	435
EtOH	24.5	1.36	0.62	375	412	434
MeOH	32.7	1.33	0.57	374	411	433
DCM	8.93	1.42	0.55	379	418	440
$CHCl_3$	4.81	1.44	0.63	380	419	441
EtOAc	6.02	1.37	0.52	375	412	435
Benzene	2.27	1.5	0.56	381	417	441
THF	7.58	1.41	0.92	378	415	437
DOX	7.2	1.42	0.91	377	415	438
n-Hexane	1.88	1.39	0.63	375	409	433
H_2O	80.1	1.33	0.34	300	418	431

Conclusion

In conclusion, we have achieved on the synthesis of a novel thiophene analogue of stilbene derivative, specifically (*E*)-1,2-bis(7-methylbenzo[1,2-b:3,4-b']dithiophen-2-yl)ethene , which may serve as a precursor to tetrathiahelicene. The synthesis has been achieved *via* McMurry coupling of 7-methylbenzo[1,2-b:3,4-b']dithiophene-2-carbaldehyde. The incorporation of the second thiophene ring is accomplished through the base-catalyzed condensation of methyl thioglycolate with 4-chloro-2-methyl-6,7-dihydrobenzo[b]thiophene-5-carbaldehyde. The Fluorescence studies reveals that in cyclic ether like THF or DOX the quantum yield of MTS is highest and it absorb at ~380 nm photon and emit with a dual peak at ~415 nm and ~440 nm.

Reference

[1] C. Thornber, *Chem. Soc. Rev.*, **1979**, *8*, 563.

[2] M. Nishioka, M. L. Lee, R. N. Castle, *Fuel*, **1986**, *65*, 390.

[3] E. Licandro, S. Cauteruccio, D. Dova, in *Thiahelicenes: From Basic Knowledge to Applications, Vol. 118* (Eds.: E. F. V. Scriven, C. A. Ramsden), Academic Press, 2016, pp. 1–46.

[4] H. Wynberg, M. B. Groen, *J. Am. Chem. Soc.* **1968,** 90 (19), 5339.

[5] K. Tanaka, Y. Shogase, H. Osuga, H. Suzuki, *Tetrahedron Letters.*, **1995,** 36 (10), 1675.

[6] J. K. Ray, S. Gupta, G. K. Kar, B. C. Roy, J-M. Lin, S. Amin, *J. Org. Chem*, **2000**, *65(24),* 8134.

[7] V. Pelliccioli, D. Dova, C. Baldoli, C Graiff, E. Licandro, S. Cauteruccio, *Eur. J. Org. Chem.*, **2021**, *3*, 383.

[8] Y. Yamashita, *Sci. Technol. Adv. Mater*. **2009,** *10(2)*, 024313.

[9] B. Kumar, B. K. Kaushik, Y. S. Negi, *Polymer Review*, **2014**, *54(1),* 33.

[10] P. Kumaresan, V. Vegiraju, Y. Ezhumalai, S. L. Yau, C. Kim, W. H. Lee, M. C. Chen, *Polymers*, **2014**, *6(10)*, 2645.

[11] Turkoglu, G.; Cinar, M. E.; Ozturk, T. *Top Curr Chem (Z)*, **2017**, *375*, 84.

[12] R. H. Martin, *Angew. Chem. internat. Edit.*, **1974**, 13 (10), 649.

[13] K. Yamada, H. Nakagawa, H. Kawazura, *Bull. Chem. Soc. Jpn*. **1986**, *59*, 2429.

[14] S. Arnaboldi, S, Cauteruccio, S. Grecchi, T. Benincori, M. Marcaccio, A. O. Biroli, G. Longhi, E. Licandro, P.R.Mussini, *Chem. Sci.*, **2019**, *10*, 1539.

[15] L. Menduti, C. Baldoli, S. Manetto, M. Bolte, H-W. Lerner, G. Longi, C. Villani, E. Licandro, M. Wagner, *Angew. Chem. Int. Ed.***, 2023**, *62*, e202215468.

[16] E. Licandro, S. Cauteruccio, D. Dova, *Adv. Heterocycl. Chem. (Eds.: E. F. V. Scriven and C. A. Ramsden), Academic Press,* **2016**, *118*, 1.

[17] S. K. Collins, M. P Vachon, *Org. Biomol. Chem.* **2006**, *4*, 2518. .

[18] B. Champagne, S. N. Labidi, *Chem. Phys. Lett.* **2016**, *644*, 195.

[19] A. Bossi, E. Licandro, S. Maiorana, C. Rigamonti, S. Righetto, G. R. Stephenson, M. Spassova, E. Botek, B. Champagne, *J. Phys. Chem. C*, **2008**, *112*, 7900.

[20] D. Dova, S. Cauteruccio, N. Manfredi, S. Prager, A. Dreuw, S. Arnaboldi, P. R. Mussini, E. Licandro, A. Abbotto, *Dyes Pigments*, **2019**, *161*, 382.

[21] C. Kim, T. J. Marks, A. Facchetti, M. Schiavo, A. Bossi, S. Maiorana, E. Licandro, F. Todescato, S. Toffanin, M. Muccini, C. Graiff, A. Tiripicchio, *Org. Electron.*, **2009**, *10*, 1511.

[22] D. Dova, L. Viglianti, P. R. Mussini, S. Prager, A. Dreuw, A. Voituriez, E. Licandro, S. Cauteruccio, *Asian J. Org. Chem.*, **2016**, *5*, 537.

[24] A. Bossi, P. R. Mussini, G. Farinola, M. Penconi, S. Cauteruccio, M. E. Thompson, E. Licandro, *Chem. Eur. J.*, **2023**, *29*, e202300339.

Chapter III: Thiophene analogue of acridine derivative: 2-methylbenzo[c]thieno[3,2-h]acridine

Introduction

Low-dimensional organic nanostructures arise from the self-assembly of pi-conjugated molecules, facilitated by diverse non-covalent interactions including hydrogen bonding, pi-pi stacking, and electrostatic attractions.[1] Most planar conjugated molecules exhibit strong fluorescence in their diluted solutions; however, this fluorescence diminishes significantly or becomes entirely non-existent in the solid state. This phenomenon can be attributed to the occurrence of self-quenching, specifically exciton-exciton annihilation, when the molecules are closely aggregated.[2-4] The investigation of Aggregation-Induced Emission (AIE) has garnered considerable attention as a means to enhance the luminescence efficiency of solid-state materials. This is of particular significance for organic devices such as OLEDs and lasers, which rely on a film or crystalline state for functionality. AIE arises from the suppression of nonradiative pathways, including vibrational and torsional energy relaxation processes, that are hindered in the aggregated state.[6-11] Polyaromatic hydrocarbons (PAHs) constitute a prominent class of organic molecules with extensive application across diverse optoelectronic domains, notably encompassing organic light-emitting diodes (OLEDs) and organic solar cells.[12-14] In contrast to benzene, thiophene exhibits superior electron-donating capabilities, consequently facilitating more efficacious charge transfer. Noteworthy advantages of thiophene-based materials encompass heightened thermal stability as well as enhanced resistance to oxidation, distinguishing them from their benzene-derived counterparts.[15]

We have successfully synthesized 2-methylbenzo[c]thieno[3,2-h]acridine (MTA), a thiophene analogue of dibenz[c, h]acridine derivative,[16] as a novel polyaromatic hydrocarbon, featuring sulfur and nitrogen heteroatoms. Our synthetic methodology is unique by its short straightforward and efficient thermal cyclization of chlorovinylimene derivative that can be easily obtained by reaction of the common chloraldehyde (**1**) (as used in previous chapters) and 1-naphthylamine. Thermolysis of chlorovinylimine with or without solvent is a general method for synthesis of polycyclicazaarenes as developed by Kar. *et. al.*[16, 17]

There are several reports on the intrinsic fluorescence of PAH molecules like pyrene, benzo[a]pyrene, phenanthrene, anthracene.[18-19] UV-visible spectroscopy and fluorescence studies are more sensitive for the detection of carcinogenic, mutagenic and highly pollutant

PAH molecules in the microgram level.[20] Our synthesized MTA also gives fluorescence emission in diverse polar and non-polar solvents primarily centered around 400 nm (I_1), 420 nm (I_2), and 440 nm (I_3). Notably, these emissions exhibit a moderate sensitivity to solvent polarity, which can be attributed to their Intramolecular Charge Transfer (ICT) character. In this chapter we have mainly focused to unveil the interaction of MTA in differently polar pure and binary solvent system like CH_3CN-H_2O. We have also studied the reversible transformation of the system i.e. dynamic nature, upon subjecting MTA to protonation in CH_3CN with TFA, the I_1, I_2, I_3 peaks disappear, and a broad peak emerges at approximately 555 nm.

Chapter IIIA: Synthesis of MTA

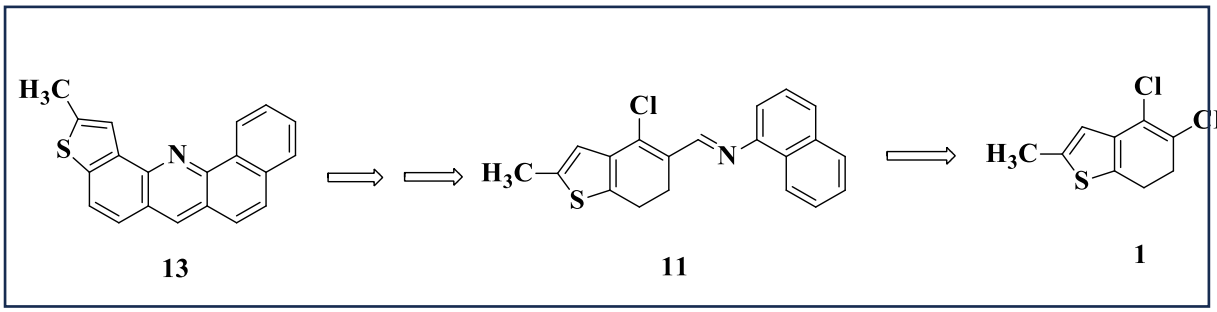

Figure 1: Retrosynthesis of 2-methylbenzo[c]thieno[3,2-h]acridine (MTA)

Numerous methods exist for synthesizing polycyclic azaarenes, including the Pfitzinger reaction,[21-22] Skraup synthesis,[23-24] Bernthsen synthesis,[25-26] and others. However, these approaches often encounter challenges in efficiently introducing electron-donating or electron-withdrawing groups into the azaarene framework. Moreover, they frequently necessitate prolonged reaction times, harsh conditions, and, notably, result in poor yields. Addressing these limitations, the Ray and Kar group has pioneered the use of thermolysis of anil hydrochlorides[27-28] and chlorovinyl imines[29-30] for synthesizing polycyclic azaarene derivatives, starting with suitable β-halo-α,β-unsaturated aldehydes. This method offers distinct advantages, including the ready availability of starting materials, shorter reaction times, high yields, and the flexibility to introduce various substituents such as alkyl, halo, nitro, alkoxy, ester, etc. In our current study, we have taken up the synthesis of a novel benz[c]acridine derivative fused with a thiophene moiety. The retrosynthesis of the molecule in **Figure 1** suggests that chloraldehyde (**1**) could serve as a suitable substrate for the synthesis of the target compound.

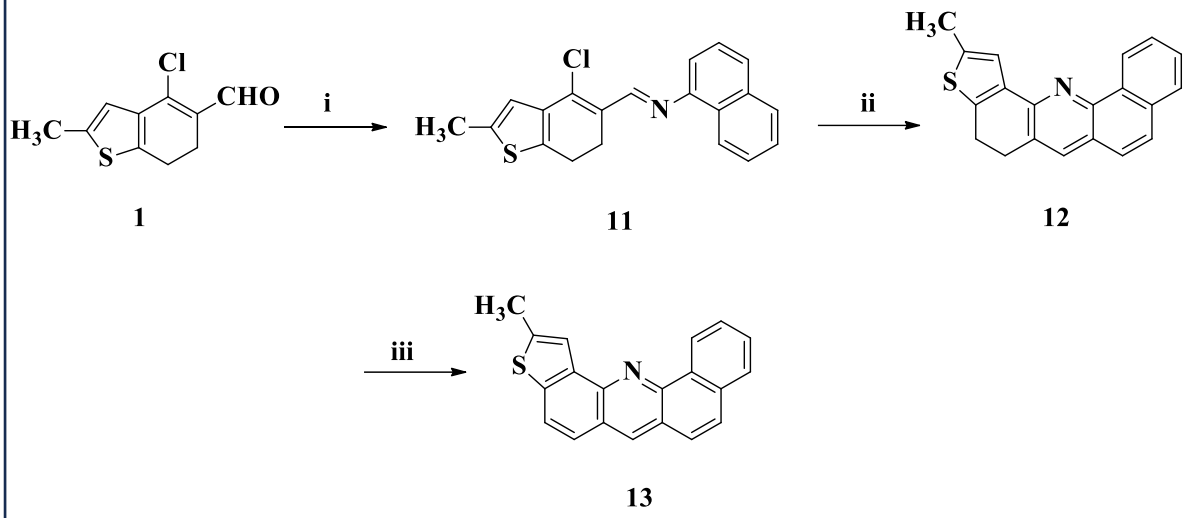

(i) 1-naphthylamine / C_6H_6, reflux, 15 hrs, (88 %) (ii) dry DMF, *p*-Toluene sulfonic acid (PTS) (*cat.*), reflux, 8 hrs, (74 %) (iii) DDQ / dry C_6H_6, reflux, 4 hrs, (90 %).

Figure 2. Synthesis of 2-methylbenzo[c]thieno[3,2-h]acridine (MTA)

The chloraldehyde (**1**) which was obtained by following a standard procedure as mentioned in early chapters,[31-32] was then treated with 1-naphthylamine in benzene under refluxing for 15 hrs and the chlorovinyl imine (**11**) was obtained as bright yellow solid in 88 % yield. The structure of the compound was confirmed by ^{1}H NMR data (400 MHz)($CDCl_3$): δ 2.48 (s, 3H) ,2.99 (t, 2H, J ~ 8.5 Hz) , 3.23 (t, 2H, J ~ 8.5 Hz), 6.93 (s, 1H) , 7.06 (d, 1H, J = 7.2 Hz) , 7.44 - 7.52 (m, 3H) , 7.71 (brd, 1H, J ~ 9 Hz), 7.84 (brd, 1H, J ~ 8 Hz), 8.33 (dd, 1H, j= 4 Hz and 7 Hz), 8.84 (s, 1H) ppm. In HRMS data two distinct *m/z* peaks correspond to the [M^++H] and [M^++H+2] was found at 338.0859 and 340.0859 respectively against the calculated values of 338.0772 and 340.0772. The [M^++H+2] peak assure the presence of Cl atom in **11**. Thermal cyclization of the imine (**11**) in refluxing dry DMF in presence of catalytic *p*-toluene sulfonic acid (PTS) for 8 hrs furnished dihydro MTA (**12**) in 74% yield. The structure of the compound **12** was assigned and characterized by the usual spectroscopic data (^{1}H-NMR, ^{13}C-NMR and HRMS data). The cyclization also can be achieved by the thermolysis of **11** in solvent free condition in lesser time but the yield is only 43% yield after usual work up and also quality of the product was very poor. In NMR (400 MHz) the methyl protons appeared at δ 2.57 ppm as singlet. The 2 x CH_2 protons respectively appeared as two triplets (J = 7.2 Hz) at δ 3.05 and 3.25 ppm. The H_6 proton appeared as a singlet at δ 7.89 ppm, while H_{12} appeared as doublet at δ 9.39 ppm. Two doublets at δ 7.62 (J = 7.6 Hz) and 7.87 (J = 7.6 Hz) ppm accounts for the

two proton signals H_7 and H_8. Rest of the four protons appeared at δ 7.63-7.73 ppm as overlapping multiplate. The aromatization of the dihydro derivative (**12**) was executed by refluxing the compound with DDQ in anhydrous benzene. The compound (**13**) was obtained as light yellow solid in 90 % yield. The compound showed the following splitting pattern in NMR spectra (400 MHz); ($CDCl_3$): δ 2.79 (s, 3H) ,7.72-7.82 (m, 5H) ,7.91 (brdd, 1H, J =8, 1.2 Hz) 7.86 (d, 1H, J ~ 8.6 Hz), 8.34 (s, 1H), 8.67 (s, 1H) , 9.64 (brdd, 1H, J = 8.4 and 1.2 Hz) ppm. HRMS data (ESI, 70 eV): m/z $[M+H]^+$ calculated for $C_{20}H_{14}NS$: 300.0849; found: 300.0846 supported the assigned structure.

Chapter IIIB: Fluorescence studies of MTA in pure and binary solvents

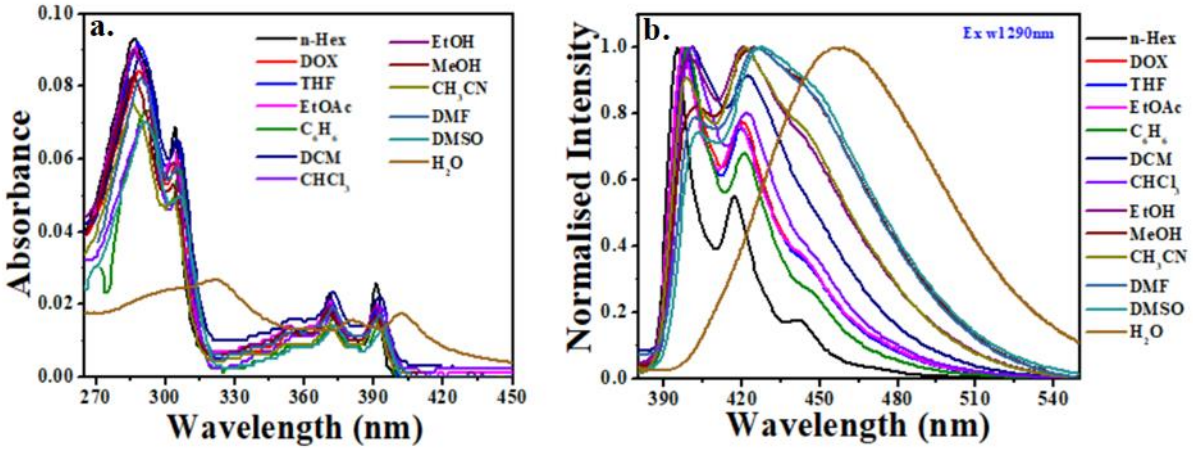

Figure 3. a. absorption spectra of MTA (2 μM) **b**. Normalized emission spectra of MTA (2 μM) in n-hexane (n-Hex), 1,4-dioxane (DOX), tetrahydrofuran (THF), ethylacetate (EtOAc), benzene (C_6H_6), 1,2-dichloromethane (DCM), chloroform ($CHCl_3$), ethanol (EtOH), methanol, acetonitrile (CH_3CN), N, N-dimethylformamide (DMF), dimethylsulfoxide (DMSO), water (H_2O).

Steady state absorption, emission spectra were measured in different non-aqueous solvent and in water (**Figure 3**). In different non-aqueous solvents, the change of the absorbance maxima with the polarity of the solvents are almost same (Table 1). In n-hexane the main absorption peak appeared at 286 nm whereas in DMSO it is centered at 291 nm but the spectral patterns are same in all non-aqueous solvents. The solvent polarity does not have a strong effect on the ground state. In water the spectral pattern are slightly different and the main absorption peak shifted to 320 nm and also an overall red shift observed in the absorbance profile. Hydrophobic

planar MTA in aqueous medium may experience a strong hydrophobic interaction which leads to form conventional J-type of aggregation.[33]

Table 1. Quantum yield, solvent parameter and spectral data of MTA in different solvents.

Solvents	Dielectric constant	Absorbance maxima	I_1 maxima	I_2 maxima	I_3 maxima	Quantum yield
DMSO	46.7	291	402	425	455	0.10
DMF	36.7	289	401	422	451	0.16
CH_3CN	37.5	286	398	419	447	0.18
EtOH	24.5	286	399	418	446	0.17
MeOH	32.7	286	400	420	451	0.14
DCM	8.93	289	400	418	443	0.21
$CHCl_3$	4.81	291	400	418	440	0.26
EtOAc	6.02	291	397	416	440	0.23
C_6H_6	2.27	286	399	417	441	0.30
THF	7.58	288	398	416	440	0.27
DOX	7.2	288	398	417	441	0.18
n-Hex	1.88	286	395	415	442	0.23
H_2O	80.1	320	-	-	464	0.09

We have also investigated the aggregation effect using precipitation method involving different percentage of water to acetonitrile solvent. In the **Figure 4** the absorbance spectra show negligible change up to 60% (v/v) water in acetonitrile beyond that the absorbance decreased and again increased when the water percentage is greater then 80%. The absorbance pattern was also changed

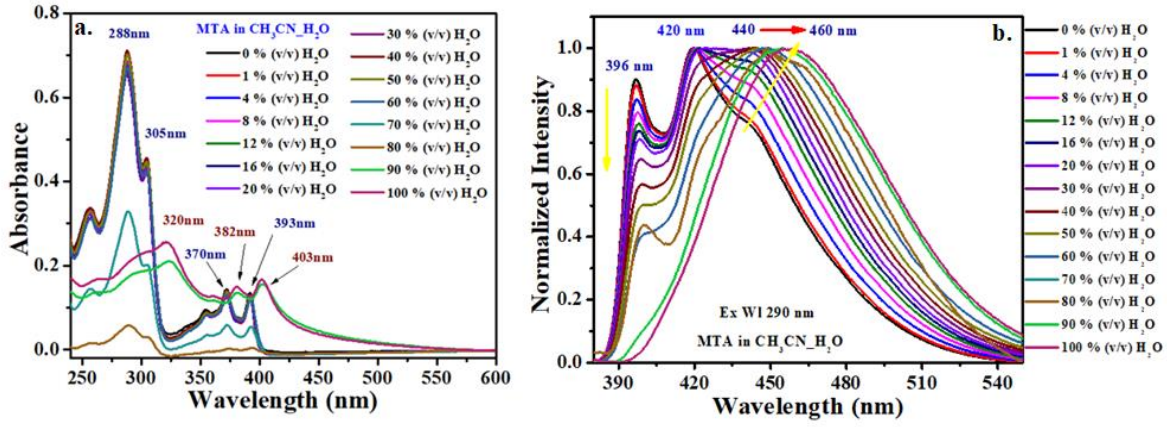

Figure 4. a. Absorbance spectra and b. emission spectra of MTA in different percent of water to acetonitrile solvent.

and almost 10 nm red shifted. The percent of aggregated formed become significant beyond 60% (v/v) H_2O and it is dominated when the volume of water exceed 80 %. The unstructured broad emission at 464 nm in water is mainly responsible for the absorption of 320 nm photon and the emissive species form in the ground state are totally different then in the emissive species in the non-aqueous solvents. The emission profile with increasing water volume percent are same in water- acetonitrile, water-ethanol and water-DMSO system (**Figure 5**) indicate the aggregation is primary responsible for the hydrophobic interaction.

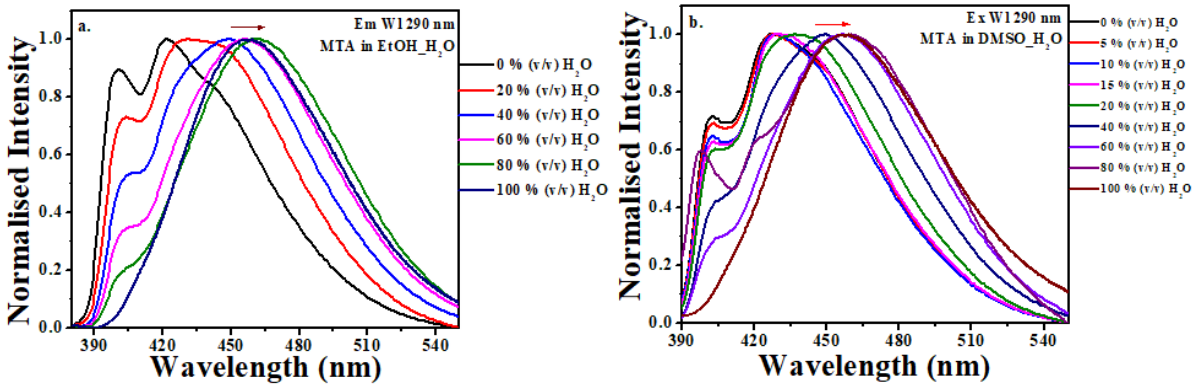

Figure 5. Normalised emission spectra of MTA in different percent of water to **a**. ethanol (EtOH_H_2O) and **b.** dimethylsulfoxide (DMSO_H_2O) solvents.

Chapter IIIC: Fluorescence studies of acidochromic behaviour of MTA

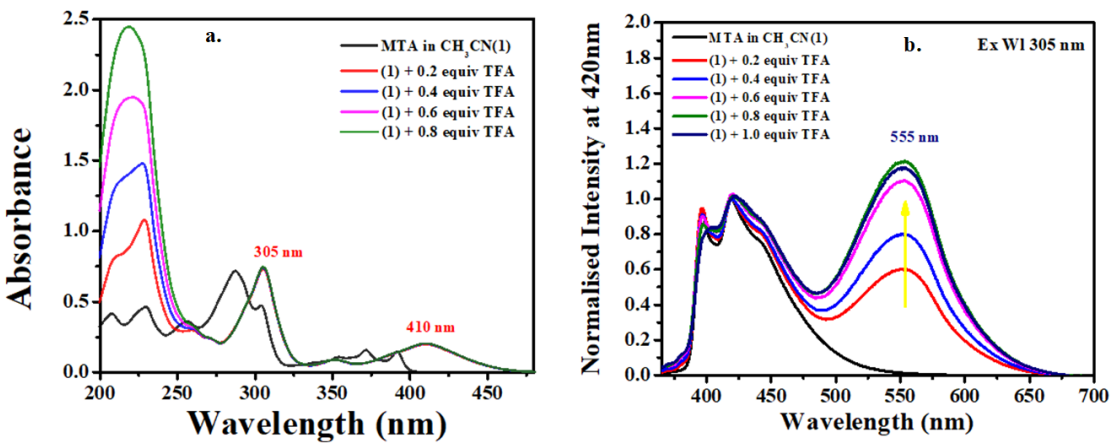

Figure 6. a. Absorbance spectra and **b.** emission spectra of MTA in acetonitrile solvent with varing trifluoracetic acid (TFA) concentration.

In this Chapter, our focus has centered on exploring the interplay between a newly synthesized thieno-acridine derivative (MTA) with strong base trifluoracetic acid (TFA). Addition of trifluoracetic acid (TFA) to MTA in CH_3CN medium a new redshifted broad emission appears at 555 nm concominent disappearance of I_1, I_2 and I_3 along with the new red shifted absorption (Figure 6). Under UV illumination the blue colored solution become bright green on TFA addition and the blue colored reappear upon addition of equivalents amount of strong base Triethylamine (TEA) (**Figure 7**).

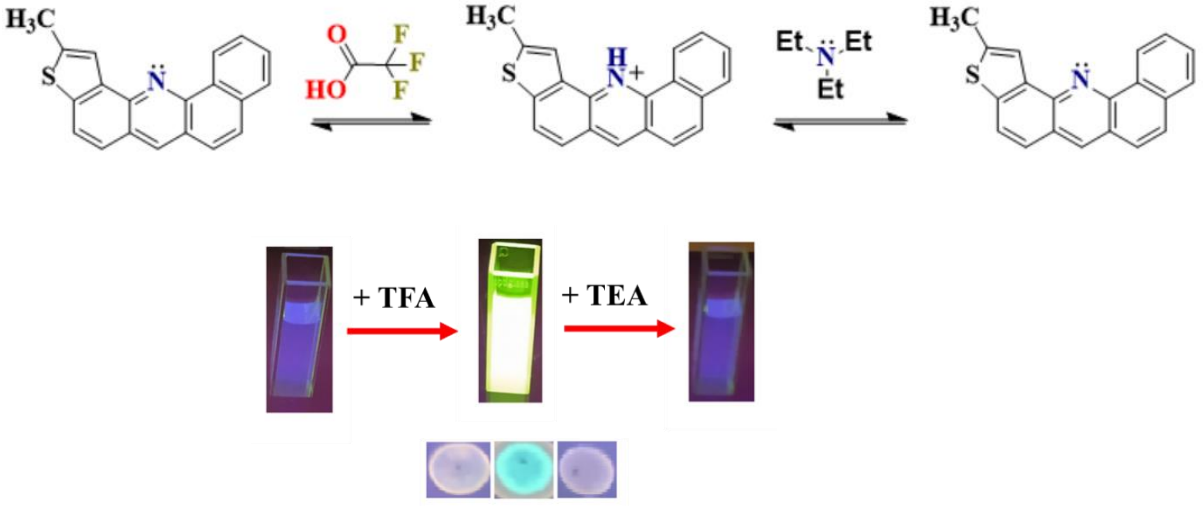

Figure 7. Acidochromic behavior of MTA

Conclusion

A newly synthesized 2-Methylbenzo[c]thieno[3,2-h]acridine (MTA) has been considered to unveil its fluorescence properties in different pure and binary solvent medium. With increasing the solvent polarity, the broad I_3 (450 nm) peak become more prominent and in binary solvents (CH_3CN-H_2O) with increasing water percent I_3 emission red shifted with concomitantly decrease of I_1 (400 nm) and I_2 (420 nm) peaks and become unstructured and broad in pure water medium. Also, in binary solvents mixture MTA exhibit an equilibrium with aggregated-non aggregated form. With increasing water percent, the hydrophobic MTA form J-types of

aggregation but the non-aggregated molecule emit mainly from the ICT state with red shifted emission centre due to high dielectric properties of the water. Upon subjecting MTA to protonation in CH_3CN with TFA, the LE and ICT-related peaks (I_1, I_2, I_3) disappear, and a broad peak emerges at approximately 555 nm, underscoring the dynamic behavior of the system.

References

[1] A. Mishra, C.-Q. Ma, P. Bäuerle, *Chem. Rev*., **2009**, *109 (3),* 1141–1276.

[2] B.-R. Gao, H.-Y. Wang, Y.-W. Hao, L.-M. Fu, H.-H. Fang, Y. Jiang, L. Wang, Q.-D. Chen, H. Xia, L.-Y. Pan, Y.-G. Ma, H.-B Sun, *J. Phys. Chem. B*, **2010**, 114 (1), 128−134.

[3] M. E. Cinar, T. Ozturk, *Chem. Rev.*, **2015**, *115 (9)*, 3036-3140.

[4] S. C. Rasmussen, S. J. Evenson, C. B. McCausland, *Chem. Commun.*, **2015**, *51*, 4528-4543.

[5] J. Chen, C. C. W. Law, J. W. Y. Lam, Y. Dong, S. M. F. Lo, I. D. Williams, D. Zhu, B. Z. Tang, *Chem. Mater.*, **2003**, *15*, 1535.

[7] Y. Ren, J. W. Y. Lam, Y. Dong, B. Z. Tang, K. S. Wong, *J. Phys. Chem. B*, **2005**, *109*, 1135.

[8] B. K. An, S. K. Kwon, S. D. Jung, S. Y. Park, *J. Am. Chem. Soc.*, **2002**, *124*, 14410.

[9] Z. Q. Xie, B. Yang, F. Li, G. Cheng, L. L. Liu, G. D. Yang, H. Xu, L. Ye, M. Hanif, S. Y. Liu, D. G. Ma, Y. G. Ma, *J. Am. Chem. Soc.*, **2005**, *127*, 14152.

[10] Y. P. Li, F. Li, H. Y. Zhang, Z. Q. Xie, W. J. Xie, H. Xu, B. Li, F. Z. Shen, L. Ye, M. Hanif, D. G. Ma, Y. G. Ma, *Chem. Commun*., **2007**, 231.

[11] Y. Ren, Y. Q. Dong, J. W. Y. Lam, B. Z. Tang, K. S. Wong, *Chem. Phys. Lett*., **2005**, *402*, 468.

[12] Y. Yamashita, *Sci. Technol. Adv. Mater*. **2009,** *10(2)*, 024313.

[13] B. Kumar, B. K. Kaushik, Y. S. Negi, *Polymer Review*, **2014**, *54(1)*,33-111.

[14] P. Kumaresan, V. Vegiraju, Y. Ezhumalai, S. L. Yau, C. Kim, W. H. Lee, M. C. Chen, *Polymers*, **2014**, *6(10)*, 2645-2669.

[15] G. Turkoglu, M. E. Cinar, T. Ozturk, *Top Curr Chem (Z)*, **2017**, *375*, 84.

[16] G. K. Kar, I. Sami, J. K. Ray, *Chemistry Letters*, **1992**, *9*, 1739.

[17] P. Patra, *J. Heterocycl. Chem*. **2017**, *54 (6)*, 3656-3662.

[18] F. Qazi, E. Shahsavari, S. Prawer, A. S. Ball, S. Tomljenovic-Hanic, *Environmental Pollution*, 2021, *272*, 116010.

[19] J. Ji, M. Jiang, Y.Zhang, J. Hou, S. Sun, *Food Reviews International*, **2023**, *39(9)*, 6977-7003.

[20] A. M. Rivera-Figueroa, K. A. Ramazan, B. J. Finlayson-Pitts, *J. Chem. Educ.*, **2004**, *81(2)*, 242.

[21] W. Pfitzinger, *J. Prakt. Chem.*,**1886**, 33(2),100.

[22] W. Pfitzinger, *J. Prakt. Chem*., **1888**, *38*, 582.

[23] Z. H. Skraup, *Berichte*, **1880**, *13*, 2086–2087.

[24] R. H. F. Manske, *Chem. Rev*. **1942**, *30*, 113.

[25] A. Bernthsen, *Ann*., **1878**, *192*, 1.

[26] A. Bernthsen, *Ann*. **1884**, *224*, 1.

[27] G. K. Kar, A. C. Karmakar, J. K. Ray, *Tetrahedron Lett.*, **1989**, *30(2)*, 223-224.

[28] G. K. Kar, A. C. Karmakar, A. Makur, J. K. Ray, *Heterocycles*, **1995**, 41*(5)*, 911.

[29] M. K. Haldar, G. K. Kar, J. K. Ray, *Synlett*, **1997**, *9*, 1057.

[30] J. K. Ray, M. K. Haldar, S. Gupta, G. K. Kar, *Tetrahedron*, **2000**, *56(6*), 909.

[31] T. B. Maiti, G. K. Kar, *Heterocycles*, **2009**, *78(12)*, 3073 – 3080.

[32] N. P. Buu-Hoi, N. Hoan, N. H Khoi, *Recl. Trav. Chim. Pays-Bas*, **1950**, *69*, 1053.

[33] M. Más-Montoya, R. A. J. Janssen, *Adv. Funct. Mater.*, **2017**, 27(16), 1605779.

List of publications in peer reviewed journals

1. **"**Tunable Luminescence of a synthesized furophenanthraquinone derivative: Interactions with different solvents**."** Aparna Sarkar, Dinesh Kumar Pyne, **Tuyan Biswas**, Rumpa Das, Gandhi K. Kar, Arnab Halder, *Luminescence: The Journal of Biological and Chemical Luminescence*, **2020**, *35*, 709.
2. **"**Photoluminescence Amplification of Cerium Incorporated Graphene Oxide Nanoparticles by Photoinduced Reduction: A Mechanistic Study Highlighting Structural Orderness." Dinesh Kumar Pyne, Shovon Chatterjee, **Tuyan Biswas**,

Prosenjit Saha, Partha Dutta, Arnab Halder, *Journal of Luminescence*, **2021**, *235*, 118019.

3. "Interaction of Aromatic Nitro Compounds and Fluoride Ions with Photoluminescent GO-Ce Nanoparticles: Understanding the Role of Local Environment of Cerium." Dinesh K. Pyne, Soumalya Pramanik, Shovon Chatterjee, Somnath Bali, **Tuyan Biswas**, Sohini Sengupta, Arnab Halder, *ChemistrySelect,* **2022**, *7*, e202202095.
4. "Tuning of Photoluminescence of Graphene Oxide Based Nanomaterials in the UV-Visible Region: Formation of Aggregates by H-Bonding through Water Molecules." Dinesh K. Pyne, Shovon Chatterjee, Soumalya Pramanik, Prosenjit Saha, **Tuyan Biswas**, Somnath Bali, Partha Dutta, Arnab Halder, *ChemistrySelect*, **2022**, 7, e202202707.
5. "Unraveling the Interaction of Synthesized Thienoangelicin Derivative by Fluorescence Studies with Solvents, Bovine Serum Albumin and Metal Ions." **Tuyan Biswas**, Injamamul Haque, Soumili Roy, Bidisha Chakraborty, Devrani Mitra, Gandhi Kumar Kar, Arnab Halder, *ChemistrySelect,* **2023**, *8,* e202300857.

List of Oral/Poster presentation in National and International Symposium

1. Poster presentation: "**Synthesis, Characterization and Photoluminescence studies of 8-methyl 2H-thieno[2,3-H]chromen-2-one and derivatives as thiophene analogue of Angelicin derivative**." *Roy, Soumili; Biswas, Tuyan; Halder, Arnab; Kar, Gandhi Kumar* in the one day National conference on Current Challenges & Opportunities in Chemical Sciences (CCOCS-2019), Department of Chemistry, Aliah University, New Town, Kolkata-700160 on **8th August 2019** [The poster was awarded with the **3rd best poster award**].

2. Poster presentation: "**Study of Excited state proton transfer (ESPT) of 1- Naphthol in presence of an anionic surfactant (SDS) and a block copolymer (F-127) : Exploration of the copolymer surfactant interaction**" *Biswas, Tuyan; Halder, Arnab* International conference on chemical science and engineering (ICCES 2019*)* at IEM, Kolkata on **19th September , 2019.**

3. Poster presentation: "**Luminescence modulation of a synthesized furophenanthraquinone derivative in different solvents as a result of specific solvent interactions**" *Biswas, Tuyan; Halder, Arnab; Kar, Gandhi Kumar;* 4th Regional Science and Technology Congress (Southern region),2019 jointly organised by Department of Science & Technology and Bio-Technology, Govt. of West Bengal & Maulana Abul Kalam Azad University of Technology, West Bengal at Haringhata, Nadia on **23rd - 24th December, 2019.**

4. Oral presentation: "**Luminescence modulation of a synthesized furophenanthraquinone derivative in different solvents as a result of specific solvent interaction"** *Biswas, Tuyan; Halder, Arnab; Kar, Gandhi Kumar;* International Conference on Chemistry for Human Development (ICCHD-2020) at Heritage Institute of Technology, Kolkata on **9th - 11th January, 2020.**

5. Poster presentation: **"Photoluminescence amplification of cerium attached graphene oxide nanoparticles: exploration of the role of cerium"** *Pyne, Dinesh Kumar; Biswas, Tuyan; Halder, Arnab*; International seminar on Recent Advances in Chemistry and Material Science (RACMS-2020) by Indian Chemical Society at Kolkata on **2-3, 8, 15, 22 & 29th August, 2020.**

6. Oral presentation: **"The study of photophysical processes in the macromolecular environment"** *Biswas, Tuyan; Halder, Arnab; Kar, Gandhi Kumar;* International conference on Chemical and Environmental science, (ICCES 2020) at IEM, Kolkata on **19th December, 2020.**

7. Poster presentation: "**Solvent effect and metal ion sensing by synthesized novel thiophene analogue of Angelicin derivative using fluorescence study**" *Biswas, Tuyan; Halder, Arnab; Kar, Gandhi Kumar*; International seminar on Recent Advances in Chemistry and Material Science (RACMS-2022) by Indian Chemical Society at Kolkata on **30-31st July and 2-3rd August , 2022.**

8. Oral presentation: **"Synthesis of thiophene analogue of angelicin derivatives and their interaction with biomolecules, metal ions by :** International conference on Chemistry and Allied sciences (ICCAS-2022) at Warangal, India on **25th-27th August, 2022.**
9. Poster presentation: "**Interaction of Thienoangelicin Derivative with β-Cyclodextrin and Metal Ions by Fluorescence Spectroscopy**" *Mukherjee, Soumita; Biswas, Tuyan; Halder, Arnab;* One day National Symposium on "Frontiers in Chemistry: from Fundamentals to Application by Department of Chemistry, Presidency University, Kolkata on **28th March, 2023**.
10. Oral presentation: "**Investigation of Photoluminescence Features of Synthesized 2-Methylbenzo[c]thieno[3,2-h]acridine in Pure and Binary Solvent Systems"** *Biswas, Tuyan; Halder, Arnab; Kar, Gandhi Kumar*; P. C. Ray Memorial International Conference on Contemporary Ideas, Innovations & Initiatives in Chemical Sciences (CI3CS-2023) at Department of Chemistry, Presidency University, Kolkata on **23rd and 24th August, 2023.**

List of other Webinar, Conference and workshop attended

1. Workshop attended on "**The Hand on training on Crafting your Career**" conducted by IndiaBioscience team at Presidency university, Kolkata on **20th September, 2019**.
2. Participated in the international webinar on "**Physics of Nanomaterials: Synthesis and Characterization with Practical Examples**" organized by Department of Applied Sciences, KIET GROUP OF INSTITUTES on **23rd June, 2020**.
3. Participated in virtual scientific event "**WEBINAR ON FRONTIERS IN ORGANIC ELECTRONICS**" organized by Department of Chemistry, National Institute of Technology, Rourkela, Odisha on **29th June- 3rd July, 2020**.
4. Participated in the international webinar on "**COVID-19-Understanding The Real Threat To Human"** organized by Department of Clinical Nutrition and Dietetics, Women's Study Centre, St. Teresa's College (Autonomous) Ernakulam, on **3rd July, 2020.**
5. Participated in the webinar on "**Perovskite Nanocrystals: Photoluminescence and Charge Carrier Dynamics**" organized by Dept. of Chemistry, School of Basic and Applied Sciences, Adamas University on **4th July, 2020**.
6. Participated in virtual scientific event ''**WEBINAR ON FRONTIERS IN CHEMICAL SCIENCES**'' organized by Department of Chemistry, National Institute of Technology, Rourkela, Odisha on **6th-10th July, 2020.**
7. Participated in the webinar on "**Gaussian, ChemDraw and Mnova Software**" organized by Department of Chemistry, School of Advanced Science, Vellore institute of Technology, Vellore and Scube Scientific, New Delhi on **21st -22nd July, 2020**.
8. Participated in One Day Webinar on "**Advance Level Study on Chemical Sciences**" organized by Department of Chemistry, School of Sciences, Netaji Subhas Open University, West Bengal on **23rd September, 2020**.
9. Participated in "**A Three-Day National Webinar on Frontiers in Chemistry: from Fundamentals to Applications**" organized by the Department of Chemistry, Presidency University, Kolkata on **25th, 26th & 27th September 2020**.
10. Participated in "**57th Annual Convention of Chemists, 2020 & International Conference on Recent Trends in Chemical Sciences (RTCS-2020)"** organized by the Indian Chemical Society, Kolkata during **26th-29th December, 2020**.
11. Participated in the celebration of "**160th Birth Anniversary Celebration of Acharya P. C. Ray International Seminar on Recent Advances in Chemistry and Material**

Science (RACMS-2021)" organized by the Indian Chemical Society, Kolkata during **1st-8th August, 2021**.

12. Workshop attended on **Molecular Docking, Pharmacophore Modeling and Machine Learning** organised by the Bioinformat ics Division, ICMR – National Institute of Cancer Prevention and Research, Noida and Schrodinger Inc. from **15 - 16th March, 2022**.
13. Participated in the celebration of the "**99th Foundation day Celebration of the Indian Chemical Society & International Research Scholars' Meet**" organized by the Indian Chemical Society and the Department of Chemistry, University of Calcutta on **9th May, 2022**.
14. Participated in "**International Conference on Drug Discovery**" held at BITS-Pilani KK Birla Goa Campus on **10th and 11th November, 2022**.
15. Attended a training session "**Accelerating Research with Oxford University Press**" organized by Oxford University Press on **17th November, 2022**.

Tuyan Biswas

Signature of the candidate

(Tuyan Biswas)

Signature of the Supervisor

(Prof. Arnab Halder)

Prof. Arnab Halder
Department of Chemistry
Presidency University, Kolkata-700 073

Gandhi Kumar Kar

Signature of the Co-Supervisor

(Prof. Gandhi Kumar Kar)

Dr. Gandhi Kumar Kar
Professor (Rtd.)
Department of Chemistry
Presidency University, Kolkata- 700 073